Spring 2017

Power dissipation and power correlations for a retreatblade impeller under different baffling conditions

Chadakarn Sirasitthichoke
New Jersey Institute of Technology

Copyright Warning & Restrictions

The copyright law of the United States (Title 17, United States Code) governs the making of photocopies or other reproductions of copyrighted material.

Under certain conditions specified in the law, libraries and archives are authorized to furnish a photocopy or other reproduction. One of these specified conditions is that the photocopy or reproduction is not to be "used for any purpose other than private study, scholarship, or research." If a, user makes a request for, or later uses, a photocopy or reproduction for purposes in excess of "fair use" that user may be liable for copyright infringement,

This institution reserves the right to refuse to accept a copying order if, in its judgment, fulfillment of the order would involve violation of copyright law.

Please Note: The author retains the copyright while the New Jersey Institute of Technology reserves the right to distribute this thesis or dissertation

Printing note: If you do not wish to print this page, then select "Pages from: first page # to: last page #" on the print dialog screen

ABSTRACT

POWER DISSIPATION AND POWER CORRELATIONS FOR A RETREAT-BLADE IMPELLER UNDER DIFFERENT BAFFLING CONDITIONS

by
Chadakarn Sirasitthichoke

Glass-lined stirred reactors and tanks are commonly used in the pharmaceutical industry because of their corrosion resistance, ease of cleanliness and minimization of product contamination. Most industrial glass-lined tank reactors are provided with a torispherical tank bottom and a retreat curve impeller with low impeller clearance from the vessel bottom. The power, P, dissipated by the impeller is a critical process parameter to mixing processes to achieve the desired mixing effect, especially since the power per unit volume, P/V, directly controls mass transfer processes and other mixing phenomena. However, little information has been published about the power dissipation and the corresponding power number, Po. The objective of this study was to determine experimentally the impeller power dissipation in the vessel and obtain power correlations for a retreat-blade impeller under various types of baffling conditions. In this study the power, *P,* was measured in fluids of different viscosities and densities at different agitation speeds, and the non-dimensional Power Number, Po, is obtained in a scaled-down version of a typical glass-lined tank reactor for a large range of the Reynolds Number ($1<Re<400,000$) for pharmaceutical active ingredient (API) synthesis. Po depended significantly on baffling type and Reynolds number, Re. Correlating equations were obtained to predict Po as a function of Re and baffling type. These equations can be used

by the industry practitioner to optimize pharmaceutical mixing processes, especially during API synthesis in reactors.

POWER DISSIPATION AND POWER CORRELATIONS FOR A RETREAT-BLADE IMPELLER UNDER DIFFERENT BAFFLING CONDITIONS

by
Chadakarn Sirasitthichoke

A Thesis
Submitted to the Faculty of
New Jersey Institute of Technology
in Partial Fulfillment of the Requirements for the Degree of
Master of Science in Pharmaceutical Bioprocessing

Otto H. York Department
of Chemical, Biological and Pharmaceutical Engineering

May 2017

APPROVAL PAGE

POWER NUMBERS AND POWER CORRELATIONS FOR A RETREAT-BLADE IMPELLER UNDER DIFFERENT BAFFLING CONDITIONS

Chadakarn Sirasitthichoke

Dr. Piero M. Armenante, Thesis Advisor Date
Distinguished Professor of Chemical, Biological and Pharmaceutical Engineering, NJIT

Dr. Boris Khusid, Committee Member Date
Professor of Chemical, Biological and Pharmaceutical Engineering, NJIT

Dr. Sagnik Busaray, Committee Member Date
Assistant Professor of Chemical, Biological and Pharmaceutical Engineering, NJIT

BIOGRAPHICAL SKETCH

Author: Chadakarn Sirasitthichoke

Degree: Master of Science

Date: May 2017

Undergraduate and Graduate Education:

- Master of Science in Pharmaceutical Bioprocessing
  New Jersey Institute of Technology, Newark, NJ, 2017

- Bachelor of Science in Pharmaceutical Sciences
  Chulalongkorn University, Bangkok, Thailand, 2013

Major: Pharmaceutical Bioprocessing

Success is the good fortune that comes from
aspiration, desperation, perspiration and inspiration.

Evan Esar

ACKNOWLEDGMENT

I would like to express my sincere gratitude to my research advisor, Dr. Piero Armenante, for giving me a valuable opportunity to work on this challenge work and for his ongoing support, guidance and encouragement.

Additionally, I would like to specially give my appreciation to Dr. Boris Khusid and Dr. Sagnik Busaray for serving as members of my research defense committee. I sincerely appreciated their support.

Importantly, my deepest gratitude goes to my parents. Without their encouragement, I would not have the opportunity to be at New Jersey Institute of Technology.

Lastly, I would like to say thank “Myself” for working hard on my research. I am very proud of myself.

TABLE OF CONTENTS

TABLE OF CONTENTS
(Continued)

LIST OF TABLES

LIST OF FIGURES

LIST OF FIGURES
(Continued)

LIST OF SYMBOLS

C	Bottom clearance (m)
D	Impeller diameter (m)
H	Liquid height (m)
N	Rotational speed (rpm)
P_H	Power dissipation (W) from Heidolph torque measurement
P_I	Power dissipation (W) from Interface torque measurement
P_{HI}	Corrected Power dissipation (W) from Heidolph to Interface torque measurement
P	Power dissipation (W)
Po	Power number
Re	Reynolds number
T	Tank diameter (m)
ρ	Liquid density (kg/m^3)
μ	Liquid viscosity (m^2/s)
ω	Angular frequency or angular speed (rad/s)

CHAPTER 1

INTRODUCTION

1.1 Background Information

Stirred glass-lined reactors are commonly used for the manufacturing of Active Pharmaceutical Ingredients (API) in the pharmaceutical industry. A typical glass-lined reactor is equipped with a retreat-blade impeller close to the bottom and a single baffle. The use of glass lining is critical to provide corrosion resistance, ease of cleanliness, and reduces product contamination [6], but it often requires manufacturing the agitation system and the tank so that no baffles are present in the tank. Instead, baffling effects are obtained by inserting a single baffle from the reactor roof. Without baffling or with insufficient baffling, the fluid moves in a swirling motion in the tank creating a central vortex, and mixing is inefficient [13]. Installing baffles eliminates such swirling motion by breaking a vortex and ultimately improving the mixing process [10].

The typically baffling configuration commonly found in tanks and reactors used in the chemical industry consists of four vertical plates having width equal to 8 to 10% (T/12 to T/10) of the tank diameter [13] and mounted at the tank wall. Wall baffles have also drawback since cleaning can be more difficult than in an unbaffled tank, which is critical in pharmaceutical manufacturing. For the reason, a single baffle, typically a beavertail baffle, is commonly used in glass-lined reactors. The beavertail baffle is typically mounted through a nozzle in the vessel head because mounting to the side of a glass-lined vessel is difficult or impossible [6]. However, in the pharmaceutical industry unbaffled systems can

also be encountered. In addition, most industrial glass-lined tank reactors are provided with a torispherical tank bottom (dish bottom). Because of glass-lining fabrication issues, a glassed retreat curve impeller with a low impeller clearance off the tank bottom is commonly preferred in glass-lined reactors. A significant body of knowledge exists on mixing in fully baffled tanks. However, despite their common use in the pharmaceutical industry, only few studies on the performance characteristics of these impellers and configurations are available.

To achieve the desired process goals, a sufficient level of mechanical agitation system, typically achieved by rotating the impeller, must be maintained. However, only limited information is available on the power dissipated and the corresponding Power Number, Po, in glass-lined reactors, especially in torispherical-bottomed reactors equipped with a retreat blade impeller (RBI) and partially baffled configuration. There is clearly a need to obtain data for power dissipation for RBI under partially baffled system, including in fully and unbaffled system configurations as well.

1.2 Objectives

Therefore, the primary objective of this work was to determine experimentally the power dissipation P and hence the impeller Power Number Po in a torispherical-bottomed tank equipped with a retreat curve impeller under different baffling conditions including:

- fully baffled system
- partially baffled system (vessel fitted with a beavertail baffle)
- unbaffled system

In addition, another objective of this work was to regress Po versus Re data with suitable fitting functions to obtain usable Power Number correlations that could then be used in the industrial practice to predict the power dissipated in these systems.

This was achieved here by measuring the power dissipated under different baffling configurations and under different hydrodynamic regimes by an RBI in a 61-L vessel that was the actual scale-down version of the glass-lined vessels typically used for API manufacturing in the pharmaceutical industry.

CHAPTER 2

THEORETICAL BACKGROUND

The power, P, dissipated by an impeller in a stirred tank is defined as the amount of energy required per unit of time to rotate the impeller in the fluid in that tank. P strongly depends on system characteristics such as sizes and geometry of the system, including the presence of baffle, impeller type, impeller diameter, impeller speed, impeller location, tanks dimensions, and the physical properties of liquids. The power dissipated by an impeller in a mixing system is obtained experimentally from measurements of the torque applied to the impeller (Γ) and the impeller rotational speed $(\mathrm{N}, \text{in rps})$ as follows:

$$\mathrm{P} = 2\pi(\mathrm{N})\Gamma \qquad (2.1)$$

The Power Number, Po (also referred to as N_P, or Ne), is a dimensionless group used to quantify the power dissipation using a non-dimensional expression, and defined as:

$$\mathrm{Po} = \frac{\mathrm{P}}{\rho \mathrm{N}^3 \mathrm{D}^5} \qquad (2.2)$$

where P is the power dissipation, N is the impeller agiational speed, D is the impeller diameter, and ρ is the fluid density. According to Equation (2.2), the power is divided by $\rho \mathrm{N}^3 \mathrm{D}^5$ to make the power dimensionless.

Using the Buckingham Pi Theorem, the Power Number can be related to other dimensionless groups of relevance in a stirred tank such as the impeller Reynolds number ($=\rho ND^2/\mu$), the Froude number ($=N^2D/g$), and geometrical ratios such as the impeller type and geometry, baffling configurations, D/T, C/T, and H/T, as follows:

$$Po = f\left(\frac{\rho ND^2}{\mu}, \frac{N^2D}{g}, \text{baffle type, impeller type and geometry}, \frac{D}{T}, \frac{C}{T}, \frac{H}{T}, \ldots\right) \quad (2.3)$$

The Froude number is relevant only if a vortex forms in the liquid (and hence the gravity effects become important). In a fully baffled system no vortex is formed and the Froude number to be neglected.

If the geometry of the system does not change, or, if all geometrical ratios are constant during scaling-up, the geometric ratios can also be neglected. Under these conditions, the Power Number becomes only a function of the impeller Reynolds number (Re), which is defined as the ratio of inertial forces to viscous forces as follows:

$$Re = \frac{\rho ND^2}{\mu} \quad (2.4)$$

Previous work has shown that, for a baffled system, the flow regime can be described by using only the Reynolds number, as follow (13):

$Re < \sim 10$	Laminar regime or creeping flow
$\sim 10 < Re < \sim 10^4$	Transitional regime
$Re > 10^4$	Fully turbulent regime

However, it should be stressed that the Power Number depends also on the type of the impeller and baffling configuration, as well as geometric ratios, if they are altered. In conclusion, experimental power dissipation data can be reported as Po versus Re, using non-dimensional geometric variables, especially including baffling, as parameters.

CHAPTER 3

EXPERIMENTAL SYSTEM AND METHOD

3.1 Experimental Apparatus

3.1.1 Vessel Apparatus

An open, cylindrical vessel with a torisheprical bottom, similar to the dish-bottom commonly found in industrial stirred tanks, was utilized as the stirred vessel for the entirety of this work. The vessel was made of a thin (0.5 mm) fluorinated ethylene propylene co-polymer (FEP) rigid film with a refractive index of 1.338, i.e., very similar to that of water (1.333) in order to minimize any curvature effect during the experiments. The vessel had an internal diameter, T, of 450 mm and an overall height of 540 mm. The overall height included the cylindrical and torispherical bottom sections, measuring 430 mm and 110 mm, respectively. A rigid collar and lip at the top of the vessel allowed it to be suspended in a larger "host" Plexiglas square tank, with each side equal to 0.61 m, as shown in Figure 3.1. The square tank had openings at its top through which tubes were inserted. The tubes were connected in a closed-loop recirculation mode to a heating/refrigeration circulating bath with digital controller (Model 12108-20 Serial No. 107600453, Cole-Parmer, USA). The water circulating between the bath and the square tank provided precise temperature control of the water in the square tank and in the fluid inside the FEP stirred vessel.

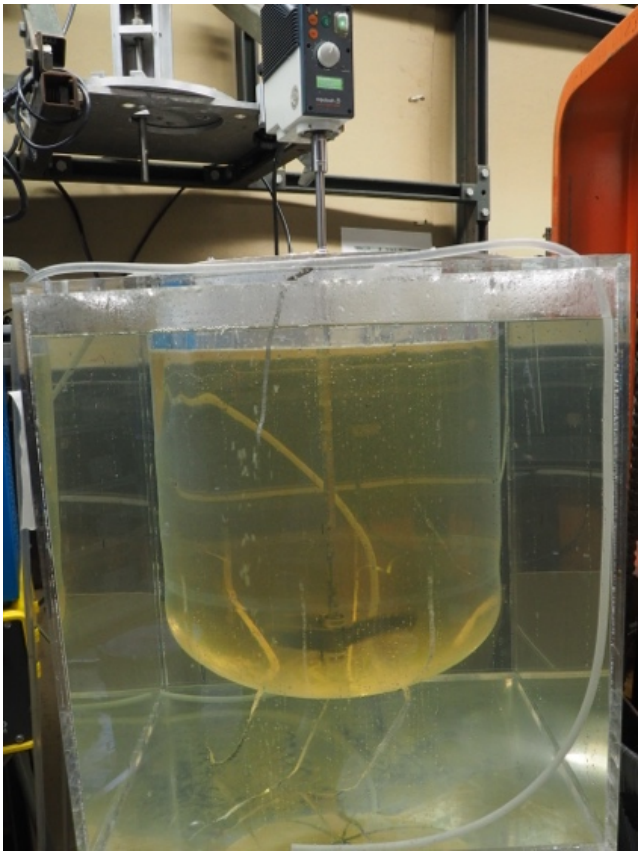

Figure 3.1 Stirred FEP vessel and host Plexiglas tank.

3.1.2 Baffling System

The stirred vessel was operated under three different baffling configurations, i.e., unbaffled, partially baffled, and fully baffled. A single beavertail baffle, shown in Figure 3.2, was used for the partially baffled system. The beavertail baffle had the following dimensions: diameter of the top section = 15.24 mm; length of the top section = 142.9 mm; diameter of the middle section = 22.23 mm; length of the middle section = 199.7 mm; diameter of the bottom section = 20.07 mm; length of the bottom section = 70.64 mm. The baffle clearance was kept constant at 182 mm, measured from the bottom of the stirred vessel. The baffle was placed midway between the center of the vessel and the vessel wall. The fully baffled system, shown in Figure 3.3, consisted of four vertical metal plates with

a width of 44 mm and a length equal to 430 mm, mounted from the top of the vessel. The lower edge of the baffles was 110 mm from the vessel bottom.

Figure 3.2 Single beavertail baffle used for partial baffling.

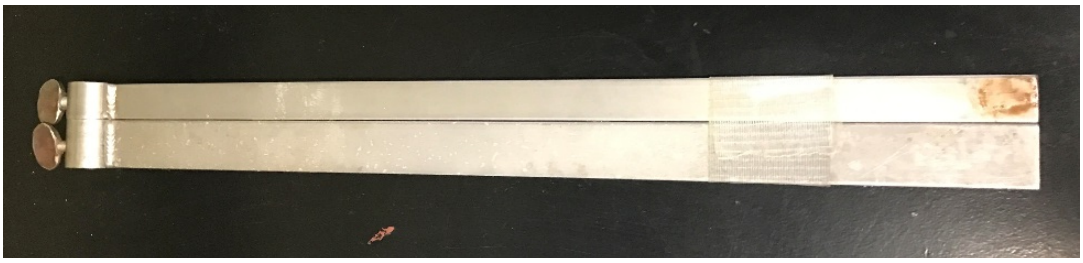

Figure 3.3 Flat baffle used for full baffling. Fours such baffle were used in the fully baffled configuration.

3.1.3 Agitation System

A single, three-blade, retreat blade impeller (RBI), geometrically similar to those typically used in commercial glass-lined vessels in the pharmaceutical industry, was used throughout all experiments. This scaled-down, aluminum impeller was manufactured locally based on the large-scale model from a commercial equipment manufacturer for the pharmaceutical and chemical industries (De Dietrich Company, Union, NJ). The dimensions of the impeller, measured with a caliper, were as follows: impeller diameter, D, = 202.5 mm; the radius of curvature of the blades = 92.08 mm; height of the blade = 25.4 mm; thickness of the blade = 12.7 mm; and an impeller diameter-to-vessel diameter ratio, D/T, of 0.487. The impeller was attached to the end of a shaft with a diameter of 12.52 mm and was centrally located inside the stirred vessel, as shown in Figure 3.4. The impeller clearance off the

vessel bottom, C_b, was always 40 mm in all the experiments. The corresponding impeller clearance-to-vessel diameter ratio, C_b/T, was 0.089, similar to the large-scale configuration.

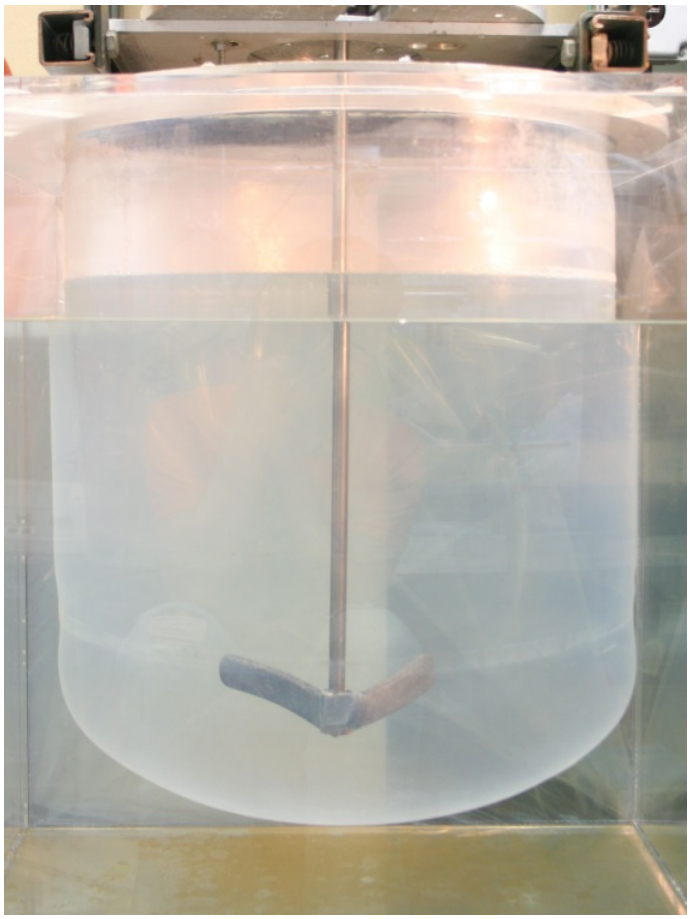

Figure 3.4 Photograph of centrally mounted impeller inside the stirred vessel.

3.1.4 Agitation Systems and Torque Measurement Apparatuses

Two different systems were used to stir the impeller and to measure the torque required to rotate the impeller in the fluid and thus determine the power dissipated in the fluid. In the first one, the impeller, coupled to an inline transducer (described below), was connected to a variable-speed, 1/3 HP Lightnin motor (Model XJ-33 VM, Serial No. 88/365321,

Lightning, Rochester, NY, USA), with a maximum rotation speed of 5500 RPM. When using this system, the torque required to rotate the impeller in the fluid and to determine the power dissipated by the impeller in the fluid was experimentally obtained using an external strain gage-based rotary torque transducer (Model, T6-5-Dual Range, Interface, Inc. Scottsdale, AZ) as shown in the Figure 3.5.

Figure 3.5 Strain gage-based rotary torque transducer.

The transducer was connected to an Interface series 9850 Multi-Channel Load Cell Indicator transferring data to a computer with M700 software (Interface) for data acquisition and processing. The transducer could measure the torque, Γ, in two different scales, i.e., 0-0.5 Nm and 0-5 Nm. Only the first scale was used in this work. The same instrument could also measure the agitation speed, N, and internally calculate the instantaneous power, P, delivered through the shaft to the impeller and the fluid, according to Equation (2.1). This system could measure torque with high accuracy (± 0.1% FS) and precision (non-repeatability=±0.02%), as specified by the manufacturer and as tested in this work, as explained below, but it could not be used effectively when the agitation speed

was low, typically below 50 rpm. Therefore, a second agitation system was additionally used, consisting of a 100 W motor (Heidolph RZR 2102 Control, range 1: 12-400 rpm, Heidolph, Schwabach, Germany) directly connected to the impeller shaft as shown in the Figure 3.6. This unit included its own internal torque meter with a torque measurement resolution of ±0.001 Nm, thus resulting in good precision. However, the accuracy of this instrument was undetermined, especially considering that the torque in this unit was internally obtained by measuring the electrical power consumed by the stirrer motor. Therefore, using this device to determine the power dissipated at the high agitation speed by the impeller required first calibrating this unit with the Interface unit, as described below, and then using the resulting calibration function to determine the power dissipation from experimental measurements.

Figure 3.6 100 W motor with accurate internal torque meter (Heidolph RZR 2102 Control).

3.2 Materials

The fluids in the stirred vessel were either water or molasses of different sugar concentrations, viscosities, and densities to vary the required density (range: 990-1589 kg/m^3), and viscosity (range: 0.6-42,000 cP), so as to explore a large range of Reynolds Number. A high-viscosity commercial molasses (Grade 42 DE Corn Syrup, Golden Barrel, www.goldenbarrel.com) was used as the initial fluid in the stirred vessel. Molasses with different viscosities were obtained by varying the fluid temperature in the square tank and hence in the stirred vessel, as well as by successively diluting the molasses with water. In such a way, the power dissipation in molasses having a large range of viscosities could be studied. The properties of the different molasses used here, each one obtained, by successive dilutions, is reported in Table 3.1. The viscosity and densities of the molasses were experimentally obtained as described below.

Table 3.1 Densities and Viscosities of Liquids at Varies Temperature Used in This Study

Liquid	Temperature, T (°C)	Density, ρ (kg/m^3)	Viscosity, μ (cP)
Molasses	30-48	1589	6,475-42,384
Molasses A	50	1416	2,807
Molasses B	50	1400	1,606
Molasses C	45	1393	1,050
Molasses D	40-45	1375	307-443
Molasses E	45.1	1364	296
Molasses G-H	27.9-39.9	1290-1308	53-96
Molasses I-J	31.5-39.1	1241-1256	19.5-22.4
Molasses K	23.6-31.9	1197-1202	9.7-15.9
Molasses L	20.5-44.3	1142	3.4-6.9
Water	16.5-43.9	990-998	0.6-1.1

3.3 Methods

3.3.1 Calibration of Torque/ Power Meters

The Interface torque/power meter was calibrated in two separate ways, i.e., statically and dynamically. The static method consisted of blocking the shaft above the inline torque transducer, mounting a disk turbine of known diameter on the shaft below the Interface transducer, applying a known force, F, to the tip of the impeller perpendicularly to the impeller diameter D, measuring the applied force with dynamometer (Shimpo FGV-0.5XY Force Gauge, 8 OZ Capacity, with a precision of ±2 N (2% high accuracy), calculating the torque from $\Gamma = F \cdot D/2$, while at the same time measuring the torque reading from the Interface torque indicator. The same procedure was repeated by applying different forces. A comparison of the torque measurements from the Interface unit with those obtained using

the dynamometer resulted in close agreement (deviation=±0.44%) over a wide range of torques (0-0.5 Nm).

Dynamic testing of the Interface torque/power meter consisted of measuring the power dissipation and hence determining the Power Number for standard 6-blade disk turbines (D= 0.1279 m) in water under turbulent conditions (Re>10,000) in flat-bottomed, baffled, Plexiglas tanks (T=0.29 m) for the typical standard configuration (C/T=0.334; D/T= 0.441), and comparing the Power Number results with the commonly reported value for such impeller, i.e., Po≅5 [1]. The results, reported in Table 3.2, show that the experimental Po value for disk turbines was 4.917±0.016, i.e., in close agreement with the literature value.

Table 3.2 The Experimental Power Number Value for Disk Turbines

Liquid Materials	**D/T**	**Agitation Speed, N (RPM)**	**Reynolds Number, Re**	**Power Number, Po, of Fully Baffled**	**Power Number, Po, from Literature** [1]
Water	0.441	119.785	26383.06987	4.83116978	5.0
		151.131	33287.0271	4.91528197	5.0
		180.482	39751.7327	4.94429875	5.0
		203.126	44739.10973	4.97816054	5.0

As for the Heidolph motor and torque meter, preliminary experiments with this system showed that the experimental power and Power Number for the RBI were is substantial agreement with those from the Interface system, but were typically smaller by a few percentage points (~5%). Therefore, some 200 separate calibration experiments were conducted with Molasses A, B, C and F in a small, flat-bottomed, baffled, cylindrical tank (T=24.20 m), in which disk turbines of different sizes (D=0.0768, 0.1030, 0.1279, 0.1529 and 0.1780 m) rotating at different agitation speeds were used, so as to vary N and P

extensively and, by changing the size of the impeller at the same agitation speed, approximately independently of each other. These experiments were repeated using the Heidolph system as well as the Interface system, and the percentage deviation of the power values in the two systems, β, defined as:

$$\beta = \frac{(P_{Interface} - P_{Heidolph})}{P_{Heidolph}} \tag{3.1}$$

The values of β were experimentally obtained as a function of N and P. The average value of β was found to be equal to 6.19%. The experimental β values were then linearly regressed using as a function:

$$\beta = a + bN + cP \tag{3.2}$$

Where N in rpm and P in W, respectively. The coefficients were found to be as follows: a= 4.2245, b= 0.0204 and c= -0.0944 (in the appropriate units). This function was found to adequately predict the experimental values of β, with an average prediction error for β of 6.5%. Therefore, when conducting actual experiments with the RBI, the Heidolph raw power consumption data was converted to the corrected power data by using the function:

$$P = P_{Heidolph} \cdot (1+\beta) \tag{3.3}$$

3.3.2 Experimental Methods to Obtain Impeller Power Dissipation Data

The molasses or water was placed to the stirred vessel, the impeller and the desired baffling system were mounted as shown in the Figure 3.7 and 3.8, the temperature in the circulation bath was set, and the system was allowed to reach the desired temperature, typically overnight.

(a) 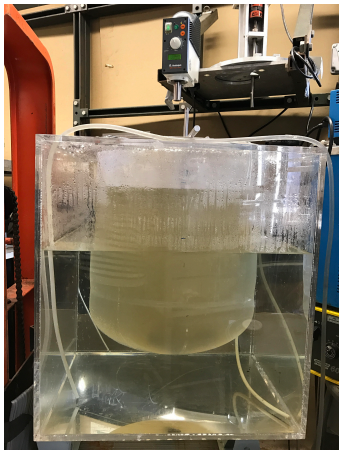 (b) 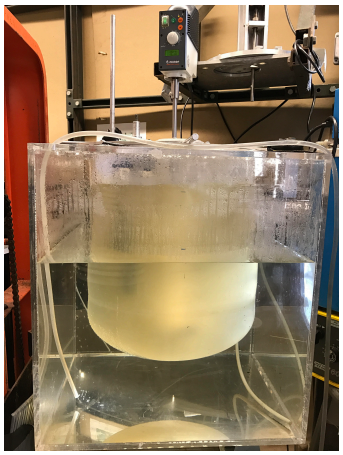 (c) 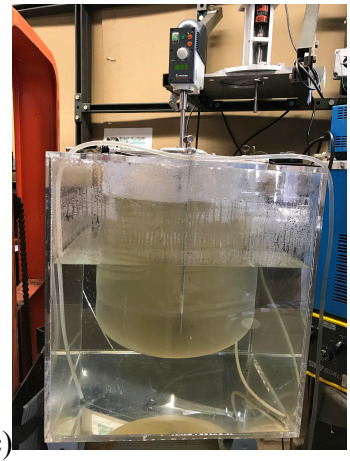

Figure 3.7 Mixing system with molasses operating under different baffling conditions:
(a) unbaffled vessel
(b) partially baffled vessel with beavertail baffle
(c) fully baffled vessel

(a) 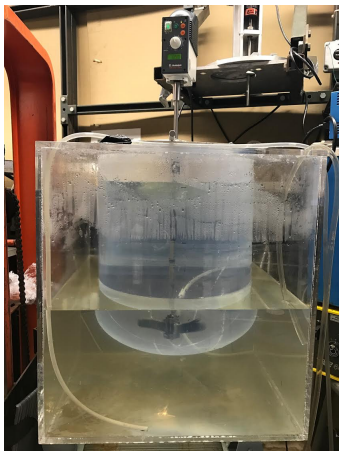 (b) 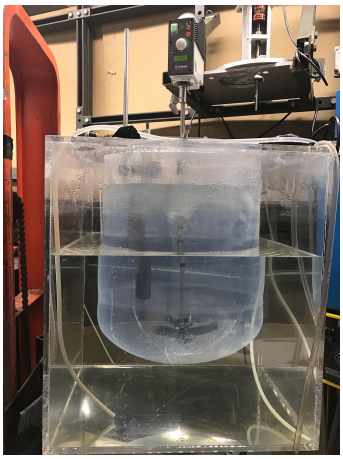 (c) 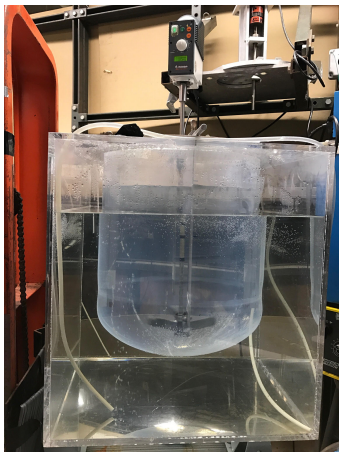

Figure 3.8 Mixing system with water operating under different baffling conditions:
(a) unbaffled vessel
(b) partially baffled vessel with beavertail baffle
(c) fully baffled vessel

Each experiment consisted of turning on agitation, allowing the system to thermally equilibrate for about an hour, and then recording the torque and/or power dissipation and the set agitation speed. Typically, ten measurements were taken when using the Heidolph unit, and the results averaged. When the Interface unit was used, the system was allowed to stabilize for 3 minutes. After steady state was reached, power data were collected for 3 minutes and averaged. Before or after an experiment the viscosity of the fluids was measured directly in the vessel, as described below, and the fluid density was measured pycnometrically by removing a sample. Some experiments were conducted in triplicate to determine the experimental reproducibility, which was found to be ±1.26%. After the experiments with a given molasses concentration were concluded, a portion of the molasses was removed, water was added water, and the system was allowed to become homogenized by stirring the vessel overnight. By varying the temperature and the water concentrations in the molasses, different fluids with similar viscosities but different water concentration

could be obtained, thus ensuring that overlapping *N-P* regions which using different fluids could be explored.

As explained before, the power, P, was experimentally determined in a wide range of Re, i.e., in both the laminar and turbulent flow regions, and Po and Re were calculated using Equations (2.2) and (2.4), respectively.

3.3.3 Experimental Methods to Determine Fluid Viscosities and Densities

Molasses and sucrose solutions are Newtonian fluids, and their viscosity could be easily measured. Since the viscosity of molasses was extremely sensitive to temperature, all viscosity measurements were conducted directly on the molasses *inside* the stirred vessel and at the same temperature of the fluid in the actual experiment, i.e., in the range 16.50-50 °C. The viscosity of highly viscous molasses, having the consistency of honey, could not be easily measured by transferring the fluid to an external viscometer without possibly altering its temperature. Therefore, for higher-viscosity molasses (2 Pa·s<μ <43 Pa·s), the viscosity was measured by dropping small steel spheres of precisely measured diameters and known densities in the unstirred molasses in the vessel. The time, *t*, for the sphere to drop by a known vertical distance, *L*, was measured (an "acceleration zone" was allowed for the sphere to reach its terminal velocity), and the viscosity was obtained from Stokes' law for the terminal velocity of a sphere falling in a fluid:

$$\mu = \frac{g(\rho_{Sphere} - \rho)d_{Sphere}^2}{18L}t \tag{3.4}$$

At a minimum, triplicate viscosity measurements were conducted. The recorded drop times were on the order of hundreds or tens of seconds, thus ensuring easy reproducibility of the test (standard deviation =±0.25)

Viscosity measurements for lower-viscosity molasses ($0.6\ 10^{-3}$ Pa·s$<\mu<2$ Pa·s), were obtained with different Cannon-Ubbelhode viscometers (Viscometer size 200, 350, and 450) immersed directly in the unstirred molasses inside the vessel, filled the same molasses, and allowed sufficient time for temperature equalization with the surrounding molasses at the temperature of the experiment to occur. Triplicate efflux time measurements in the viscometer were typically taken (standard deviation =±2.08)

The properties of water at any temperature were obtained from standard references (https://www.thermexcel.com/english/tables/eau_atm.htm). The densities of all molasses were obtained with a calibrated pycnometer.

CHAPTER 4

RESULTS AND DISCUSSION

4.1 Preliminary Results for Water

From a linear regression of the experimental calibration data with disk turbines of different diameters in flat-bottomed tanks, as described in the previous section, the experimental β values were obtained as a function of N and P, as follows:

$$\beta = (4.2244817)N + (0.02047801)P - 0.09445914 \quad (4.1)$$

where β in %, N in rpm, and P in Watts. Additional details of this regression for operating conditions in the Appendix A1. Knowing the β value enabled the data from the the Heidolph system to be harmonized with those of the Interface system.

Figure 4.1 reports the Po versus Re data obtained for water using the RBI in the fully baffled vessel. This figure shows the relationship between Po and Re in the turbulent regime that Po is very approximately equal to 0.75. This Figure also shows that the data from the Interface system overlapped with those from the Heidolph system, appropriately corrected using the β function.

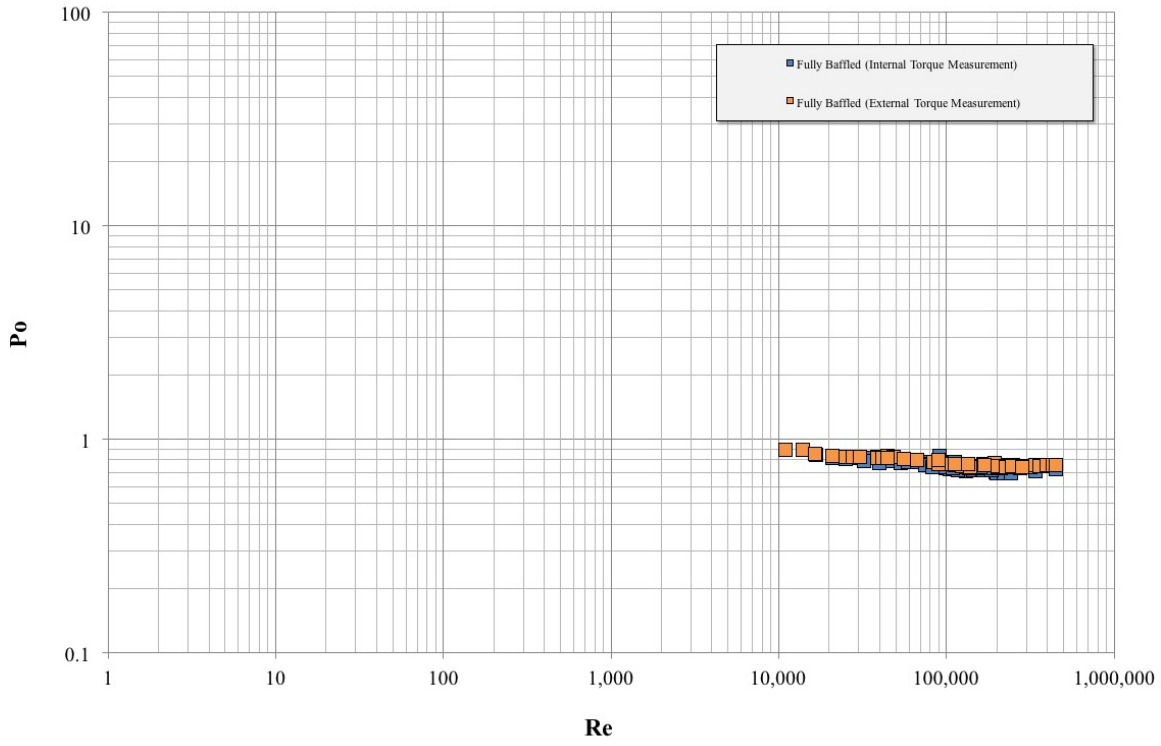

Figure 4.1 Power Number Po vs. Reynolds Number Re for water using the RBI in the fully baffled vessel. Data were obtained using both the Interface system and the Heidolph system (appropriately corrected using the β function).

Figure 4.2 presents the Po versus Re results for water obtained with the Interface system using different baffling configurations. The effect of different baffling configuration is clearly observable.

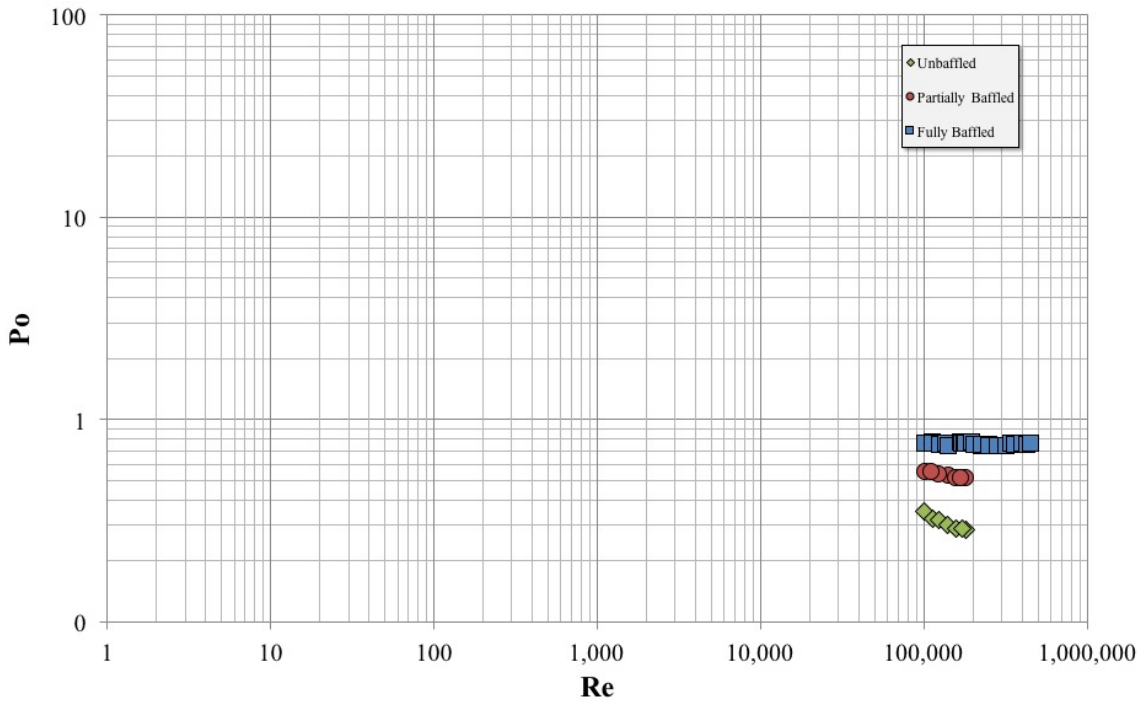

Figure 4.2 Power Number Po vs. Reynolds Number Re for water using the RBI in the stirred vessel under different baffling configurations. Data were obtained using both the Interface system only.

4.2 Power Number Curves for RBI under Different Baffling Configurations

Figure 4.3. shows the experimentally obtained values of Po as a function Re for the RBI in the fully baffled vessel for 1<Re<500,000. For Re<10, i.e., in the laminar region, the values of $\log_{10}$(Po) can be seen to vary linearly with $\log_{10}$(Re), implying that Po is inversely proportional to Re as expected [13]. For Re>4000, that is, in the fully turbulent flow regime, Po remained quite constant and nearly independent of the Re, as shown in the Figure 4.3. The liquid free surface in the fully baffled systems was observed to be nearly perfectly horizontal because of the presence of baffles that converted some of the tangential flow generated by the impeller into axial flow. The value of Po in this range was equal to 0.75. This is also expected since the Power Number for different type of impellers was reported to reach a constant value at high Re when the system was fully baffled [5].

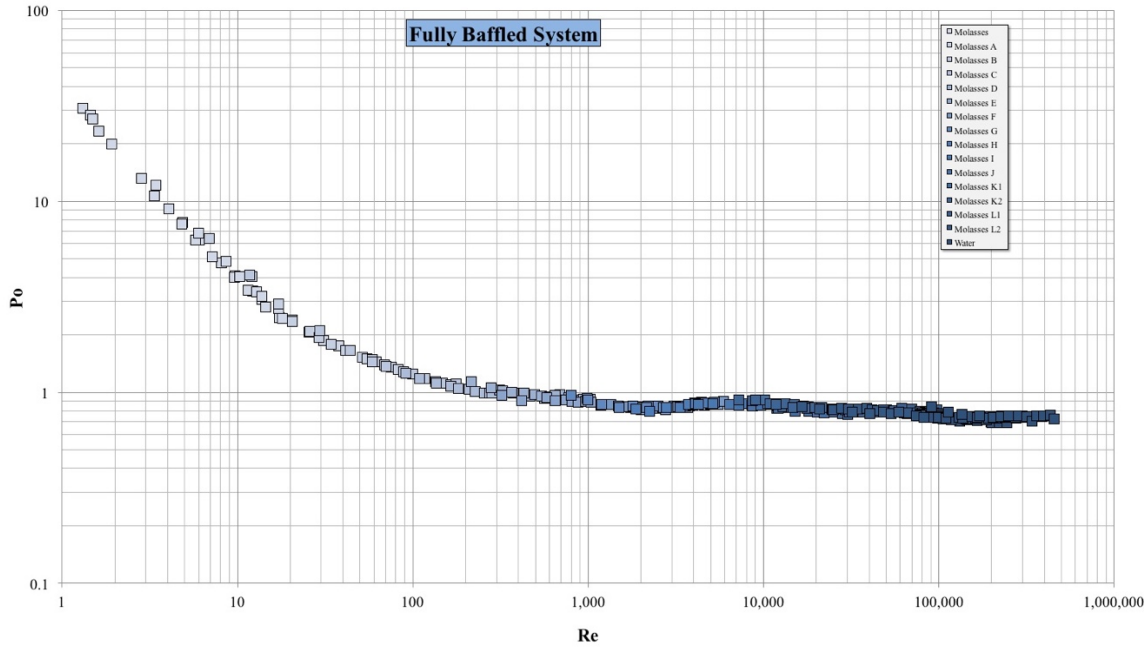

Figure 4.3 Experimental Power Number (Po) versus Reynolds Number (Re) for liquid viscosities ranging from 0.6 to 43,000 cp for the fully baffled system.

Interestingly, the Po data for Re>1,000 did not align themselves on a perfect horizontal line, but they tended to "bulge up" for Re≈10,000. There is no fundamental reason to expect that the Po value in this region should remain perfectly constant, and in fact previous investigations using other type of radial impellers have reported a similar phenomenon [3]. However, for these radial impellers, such as disk turbines and flat-blade turbines, the Po value was reported to decrease at intermediate Reynolds Number [3] before flattening out at very high Re values (>~30,000). In our case, the Po value instead went up before becoming approximately constant at high Re. In order to make sure that our data were not artifacts, the same Re range where this phenomenon occurred was investigated using molasses of different concentrations as well as using water, i.e., with solutions of very different viscosities. This in turn required using different agitation speeds to achieve

similar Reynolds numbers. In all cases, the Po values for Re≈10,000 presented a small maximum (with Po≈0.85-0.9) thus confirming that these results are correct. In 2002, Campolo, M. et al. had reported Po for a retreat blade impeller in a tank containing with two beavertail baffles was also reported to be the constant in the highly turbulent regime and with a Po value similar to that found here [5].

For the partially baffled system with a single beavertail-style baffle, Figure 4.4 shows that Po decreased with 1/Re in the laminar regime (Re<10). For higher values of Re, Po decreased linearly on a logarithmic scale, and kept slightly decreasing even when Re was larger than 100,000. These results are also in substantial agreement with those of reported by Hemrajani et al. [13], although no experimental data were ever shown in this reference or in any of the literature cited in this reference.

The liquid free surface for the partially baffled system was observed here to be also horizontal, as in the fully baffled systems, although a very small vortex formation could be observed. Therefore, in this study the liquid free surface for fully baffled and partially baffled systems was always assumed to be flat, and effect of the Froude number was neglected.

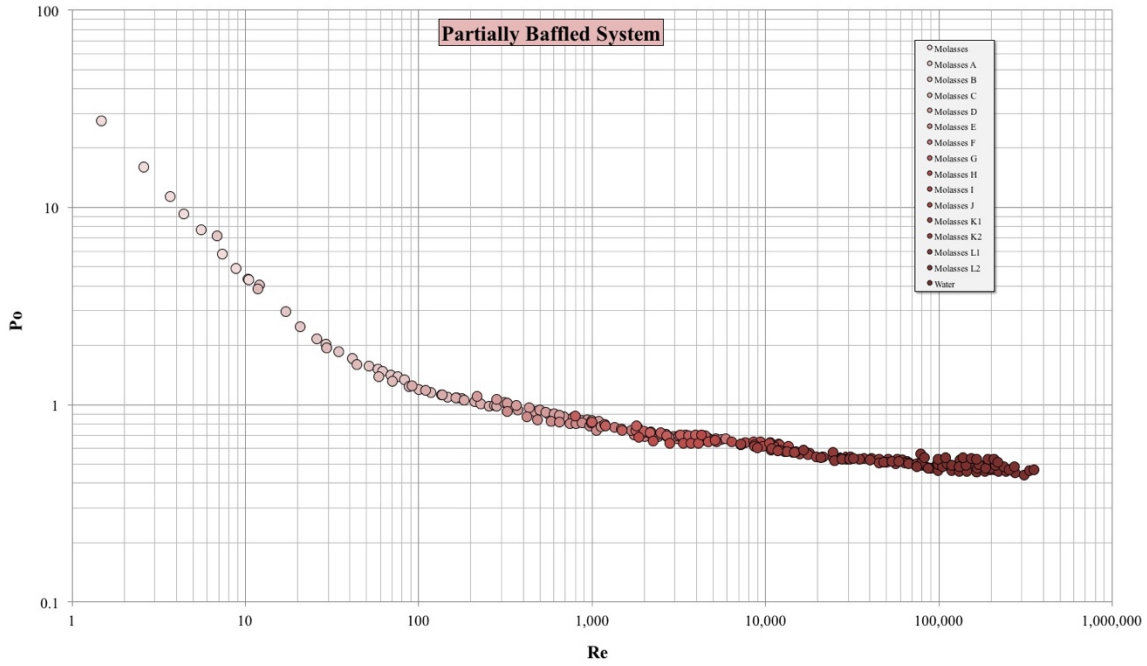

Figure 4.4 Experimental Power Number (Po) versus Reynolds Number (Re) for liquid viscosities ranging from 0.6 to 43,000 cp for the partially baffled system.

For the unbaffled system the result presented in Figure 4.5 shows that the Power Number was once again proportional to 1/Re for Re<10, as in the previous baffling configurations. However, at higher values of Re the air surface began to deform and a central vortex appeared. The vortex formation and its depth depend on the agitation speed, and very deep vortices are typically undesirable as mixing efficiency decreases and vibrations and instabilities appear [15]. In our experiments, the vortex was observed to significantly reduce the power dissipation of the system. However, in all experiments, even those at very high Re, the vortex depth never reached the impeller (i.e., the system always operated in the "subcritical" region as reported by Scargiali, F. et al., defined there as a system in which the vortex did not reach the impeller [15]). However, although Po could also depend on the Froude number, the data reported in Figure 4.5 show that Po could be just be expressed as a function of Re only. This conclusion is also consisted with that

of previous investigators [15] who reported that the Froude Number became relevant to quantify Po only when the vortex depth was equal to, or larger than, the impeller depth ("supercritical" region). Therefore, even for the unbaffled case Po was plotted as function of Reynolds number alone, which was the only variable needed here to describe Po. In 2013, Scargiali, F. et al. had also clearly reported at "subcritical" region (as defined above) Po was a weak function of Re compared to that of "supercritical" region [15].

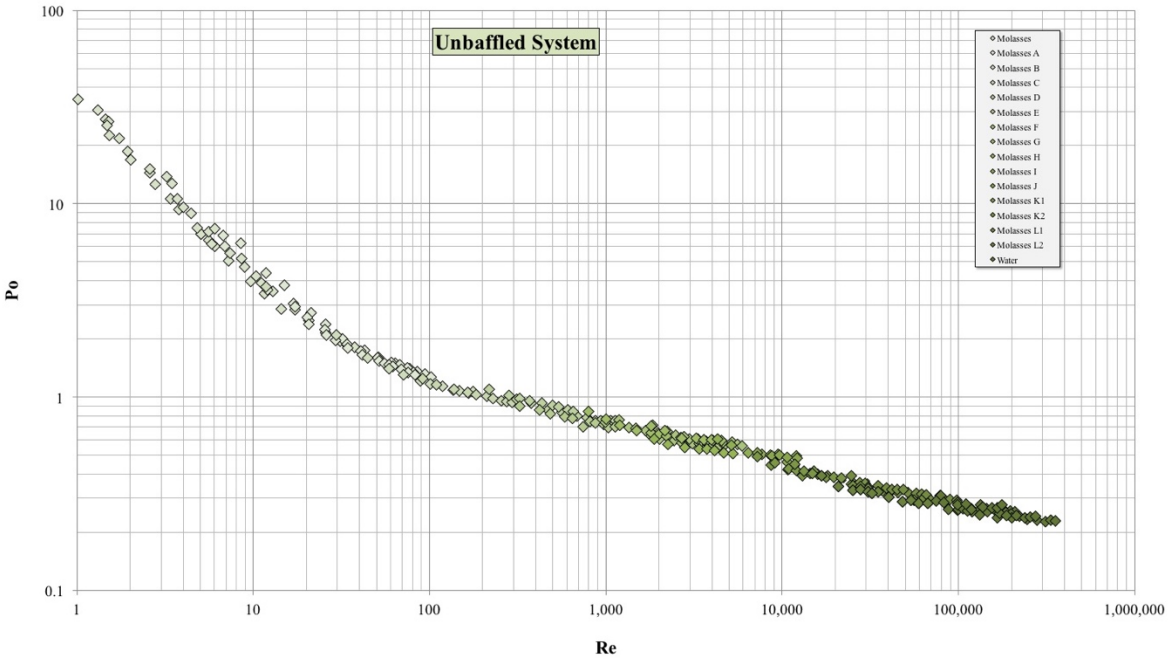

Figure 4.5 Experimental Power Number (Po) versus Reynolds Number (Re) for liquid viscosities ranging from 0.6 to 43,000 cp for the unbaffled system..

When compared together, as shown in Figure 4.6, plots of Po versus Re show that the data for different baffling conditions overlap nicely for Re<~100, which is reasonable since the presence of baffles has little impact on Po in viscous system [3, 13]. Only when Re>100 did the data start diverging.

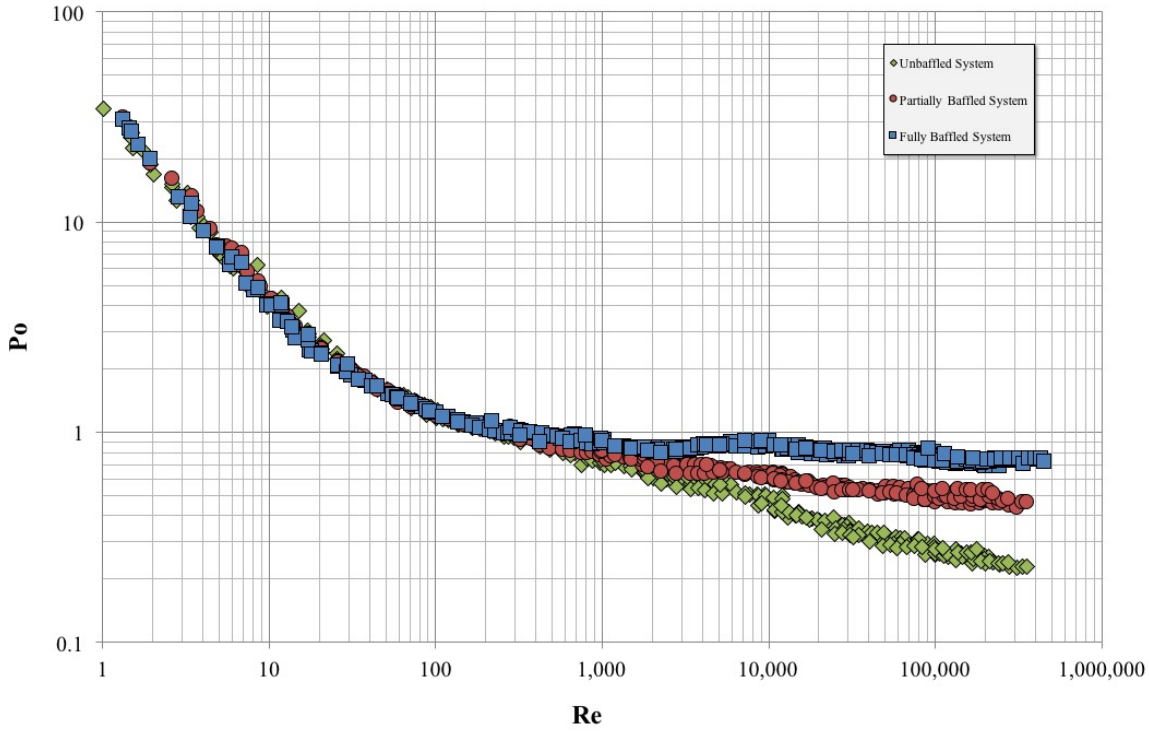

Figure 4.6 Experimental Power Number (Po) versus Reynolds Number (Re) for liquid viscosities ranging from 0.6 to 43,000 cp for different baffling configurations.

At low Re, less than about 10, the flow is laminar flow irrespective of the presence of baffles or not. In this region, the Po curves decrease for all baffling configurations when Reynolds Number is increased [12].

At high Re, greater than about 10^4, the effect of turbulence become evident, the system operates under increasingly turbulent conditions, and baffling becomes relevant. The power consumption in the presence of four wall baffles is the greatest and essentially constant at high Re. In such a case, the baffles transform tangential flow into vertical flows, thus providing more effective top-to-bottom mixing without swirl, and minimizing air entrainment. Furthermore, it is because of the baffles that drag and the power drawn by the impeller increase [8, 13]. It should be remarked that the power consumption depends

not only on the type of impellers, the agitation speed, the physical properties of the fluid, the geometry of the system but also on the baffling types. However, impeller type, agitation speed, fluids, geometry, and H/T, are similar in each of our experiments, Therefore, the differences in Po curves originate only from the different baffling types. In addition to the baffling system, the number of baffles have also a significant effect on the Po. As the number of baffles increases, Po also increases, as shown in the turbulent regime for the fully and partially baffled cases, as shown in the Figure 4.6.

4.3 Data Analysis

4.3.1 Determination of Correlating Equations

The data presented in the previous section can be used to predict the Power number and hence the power consumption in any geometrically similar system. However, this requires manually entering the value of Re to read the corresponding value of Po. It is clearly advantageous to use instead an equation adequately correlating the data so as to make the calculation of power dissipation possible *in silico*, i.e, using algorithm in computer program. Therefore, here the Po-Re data were regressed to obtain such correlations. This in turn required the selection of appropriate functions incorporating the smallest number of adjustable parameters. Two approaches were used here to derive correlations fitting the data as explained below.

Correlation Based on Modified Nagata's Equation

The first approach consisting in the use of a modified Nagata's [9] equation, and the second based on a simple power-law function. The first approach was considered here since Nagata extensively studied unbaffled, and to a limited extent, baffled systems, and

generated several semi-empirical correlations for the Power Number. Many of such correlations relied on the empirical determination of a large number of adjustable parameters to account for the effect of different geometric variables. While the use of too many adjustable parameters is less than optimal both practically and conceptually, some of his more fundamental insight can still be useful and this is why a method based on this approach was used here.

The general form of the Nagata's correlation that was used here as the starting point to relate Po versus Re for RBI in all the baffling configurations examined here is as follows:

$$Po = \frac{A}{Re} + B\left(\frac{1000 + 1.2\,Re^{0.66}}{1000 + 3.2\,Re^{0.66}}\right)^{p} \tag{4.2}$$

Nagata provided some rationale for the use of the numerical values of the constants (1000, 1.2, 3.2, 0.66) in this equation. Nevertheless the parameters *A, B,* and *p* must be determined from data regression.

In this work, we attempted not only to minimize the number of adjustable parameters (limited here to A, B and p), but also to use common values for some of these parameters irrespective of baffling whenever possible. The first term on the left-hand side of this equation (=A/Re) represents the power consumption in the laminar regime, as shown in the Equation (4.2), while the second term represents the power number in the turbulent regime. The coefficients of the correlation equation *A* and *B* were forced to be independent of baffling while *p* was allowed to vary with baffling type.

The determination of A, B and p was obtained in three steps. The first step was to calculate the value of A. To do so, one must examine for the laminar flow case, in which

case the second term on the left-hand side of the equation can be neglected and the equation reduces to:

$$Po = \frac{A}{Re} \qquad for\ Re < \sim 10 \tag{4.3}$$

Therefore, by regressing only the Po-Re data for Re < 10, the value of *A* can be obtained as the slope of Po versus Re in a logarithmic plot using all the experimental points shown in Figure 4.7. From this regression the value of 39.724 was obtained which could be more conveniently approximated to A=40 with minimal loss accuracy. It should be stressed that all $\log_{10}$(Po) vs. $\log_{10}$(Re) values aligned themselves on a straight line, irrespective of baffling type. This also implies that the term A=40 is now applicable in Equation 4.2.

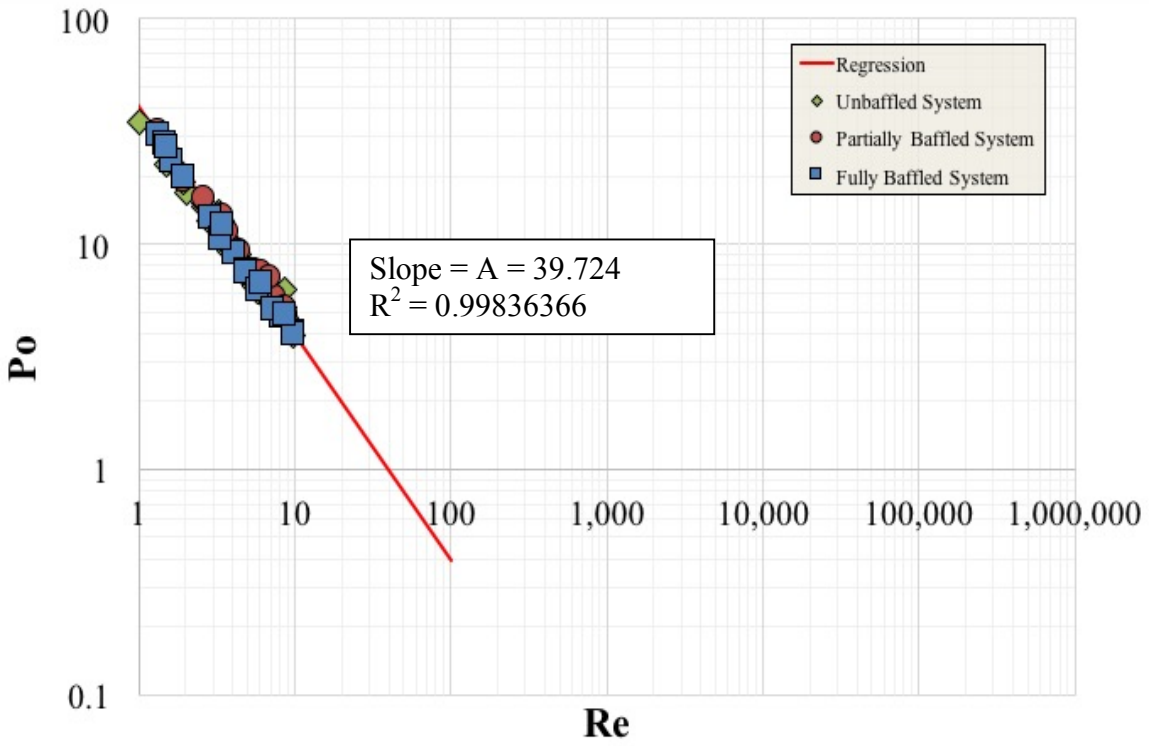

Figure 4.7 Correlation of Po vs. Re for the RBI impeller using all experimental data in the laminar regime, from which *A* can be obtained.

The second step consisted of obtaining B. To do so, only the fully baffled case was examined. Since at very high Re the value of Po must reach a constant value, then it must be that in the highly turbulent regime Po becomes independent of *p* if the system is fully baffled. Hence, *p*=0 for the fully baffled case and one can write that

$$\lim_{\boldsymbol{Re}\to\infty} Po = \frac{A}{Re} + B \text{ (fully baffled system)} \tag{4.4}$$

The asymptotic value of Po was obtained here by regressing the data for Re>40,000 for the baffled system, and was found to be equal to 0.749. Since the term A/Re is

practically equal to zero in this Re range then, from Equation 4.4, it results that B is also equal to 0.749, which can be approximated to B=0.75 with minimal loss accuracy.

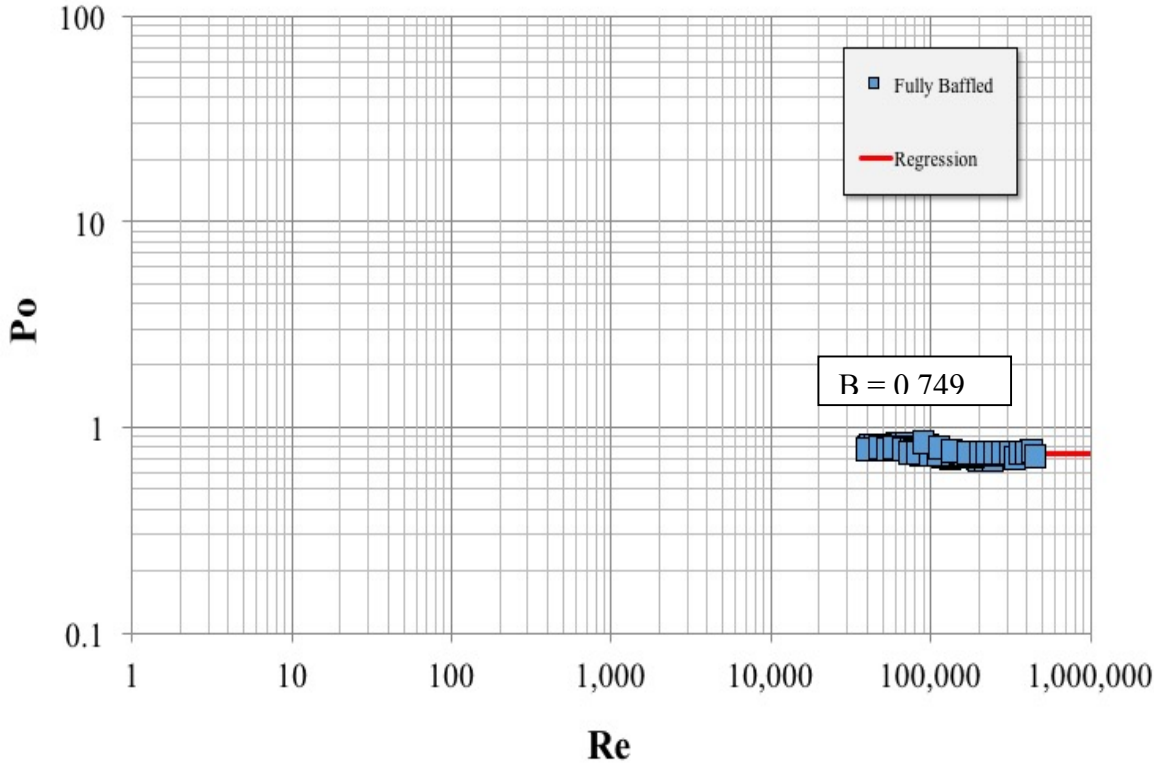

Figure 4.8 Correlation of Po vs. Re for RBI in the fully baffle system when Re=40,000, from which *B* can be obtained.

The third step consisted in determining the values of *p* for each baffling configuration while retaining the value of A=40 and B=0.75 irrespective of baffling. Accordingly, p was taken to be zero for the fully baffled case and the best fit values for *p* for each individuals baffling system configurations were obtained. The results are in Figure 4.9 , 4.10 and 4.11, respectively. The coefficient *A*, *B* and *p* for each baffling type are summarized in Table 4.1.

Table 4.1 Summary of Coefficients *A*, *B* and *p* and Their Standard Errors for Each Baffling Type Using the Modified Nagata Equation Approach

Baffling Type	A	B	p
Four baffles	39.724 ± 0.256	0.749 ± 0.002	0
Beavertail baffle	39.724 ± 0.256	0.749 ± 0.002	0.518 ± 0.005
No baffle	39.724 ± 0.256	0.749 ± 0.002	1.262 ± 0.010

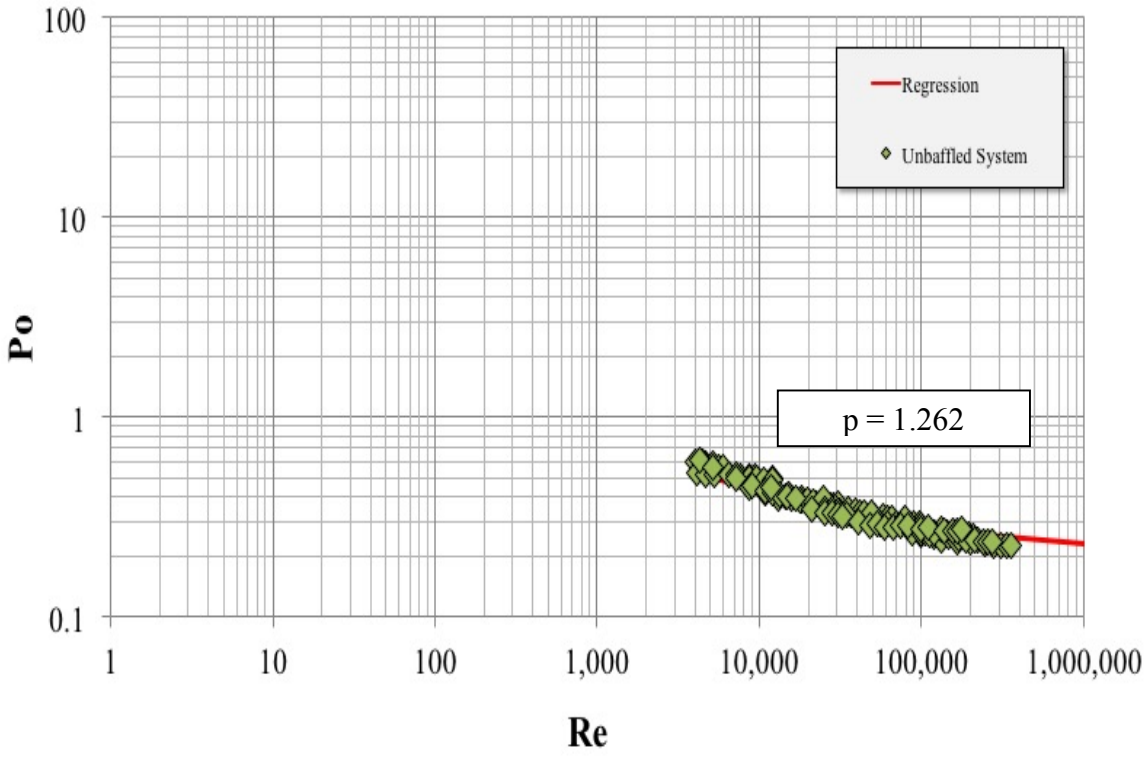

Figure 4.9 Correlation of Po vs. Re for RBI in the unbaffled baffle system for Re>4,000 from which *p* for the unbaffled system can be obtained.

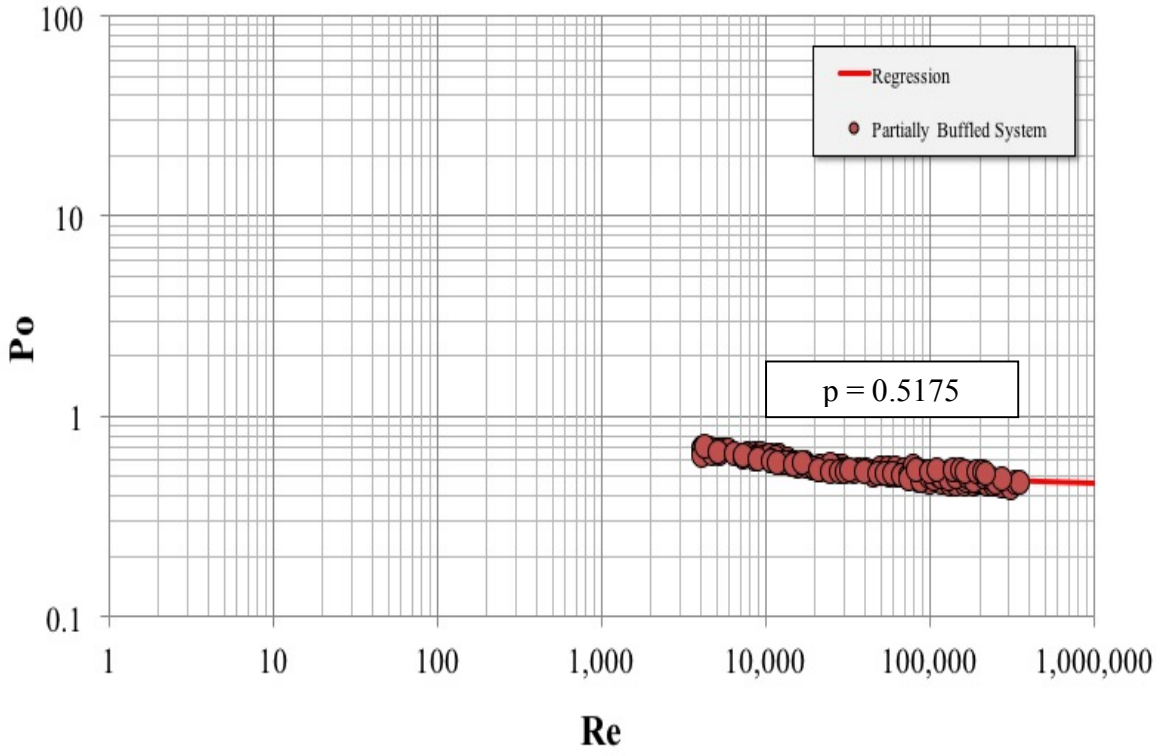

Figure 4.10 Correlation of Po vs. Re for RBI in the partially baffled baffle system for Re>4,000 from which *p* for the partially baffled system can be obtained.

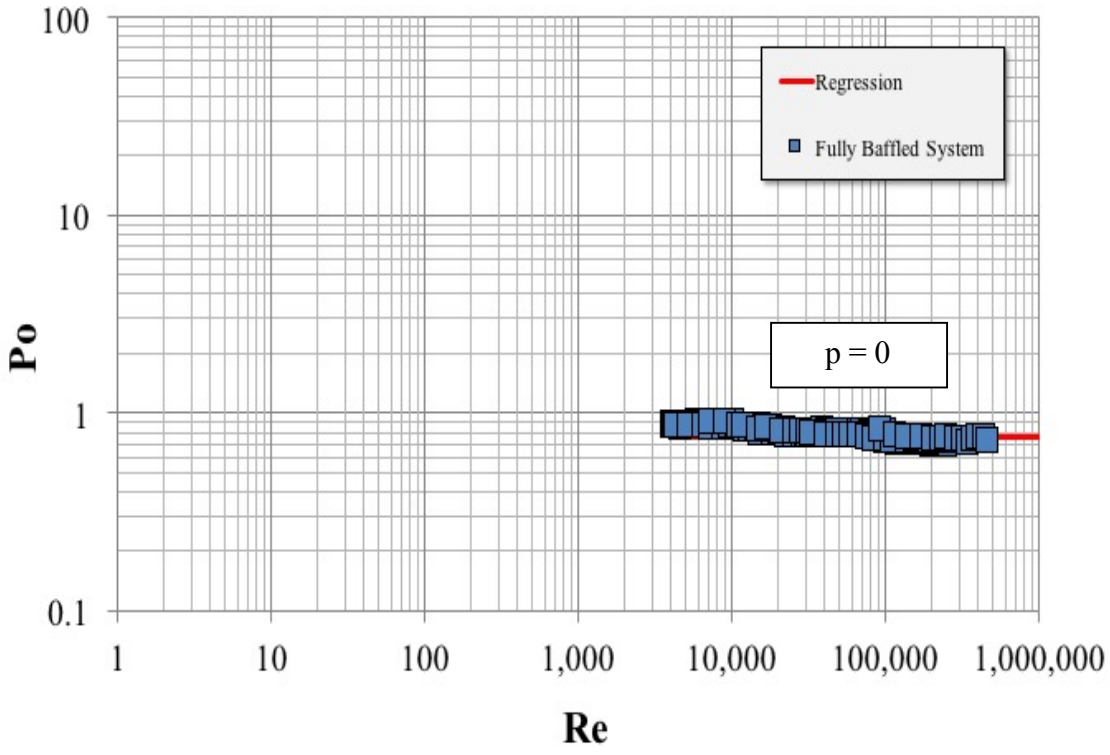

Figure 4.11 Correlation of p for retreat-blade impeller with fully baffled system.

Correlation Based on Power-Law Equation

The second approach that was used here to correlate the data was by using following general based power-law function to regress Po versus Re data:

$$Po = \frac{A}{Re} + FRe^{q} \tag{4.5}$$

where the parameters *A, F,* and q must be determined from data regression. The first term represents the power consumption in the laminar regime. Therefore, the same analysis conducted for the previous correlating equation applies and Equation 4.3 can be used, resulting again in A=40 for all cases, irrespective of baffling type.

Therefore, *A* was be independent of baffling while *F* and *q* were allowed to vary with baffling type. To obtain them knowing A, the values of (Po -A/Re) were plotted vs. Re for each baffling type, using a log-log scale, and *F* and *q* were obtained, respectively, from the intercept and slope. Again, only data for Re>40,000 were considered, to ensure good fitting in the turbulent region rather than in the transition region.

Accordingly, the best fit values for *F* and *q* for each individuals baffling system configurations were obtained as shown in the Figure 4.12 , 4.13 and 4.14, respectively. The coefficient *A*, *F* and q for each baffling type are summarized in Table 4.2

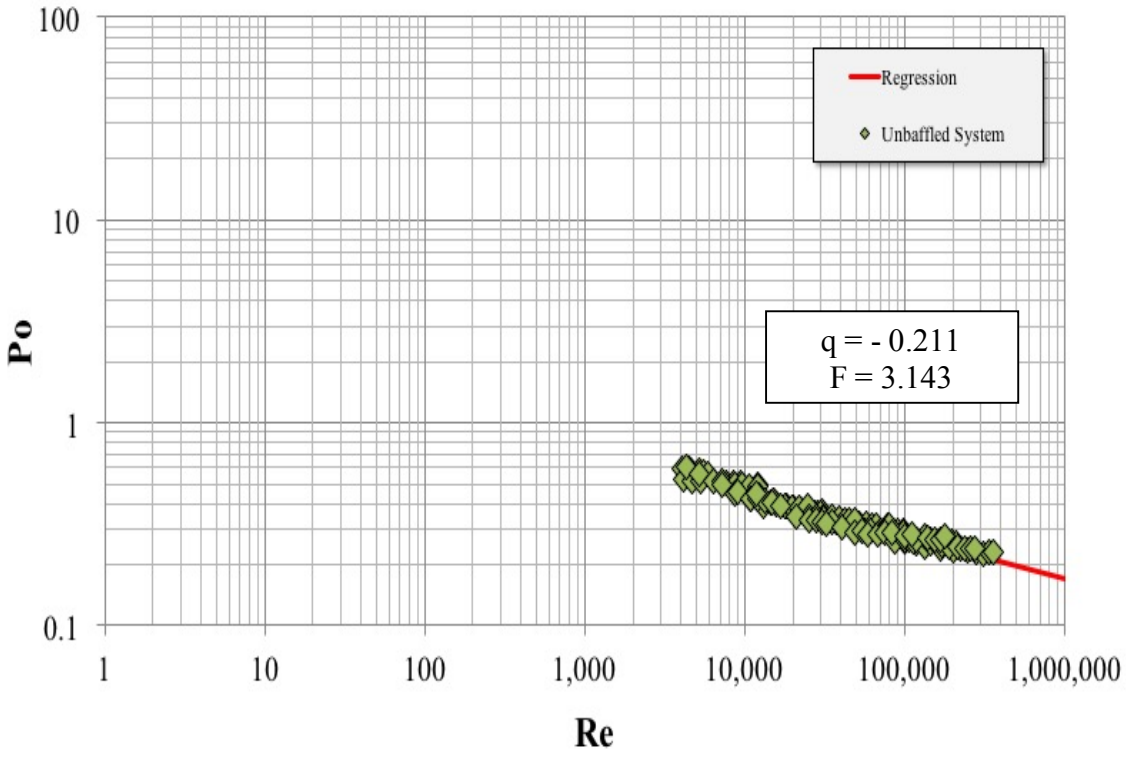

Figure 4.12 Correlation of *F* and *q* for retreat-blade impeller with unbaffled system.

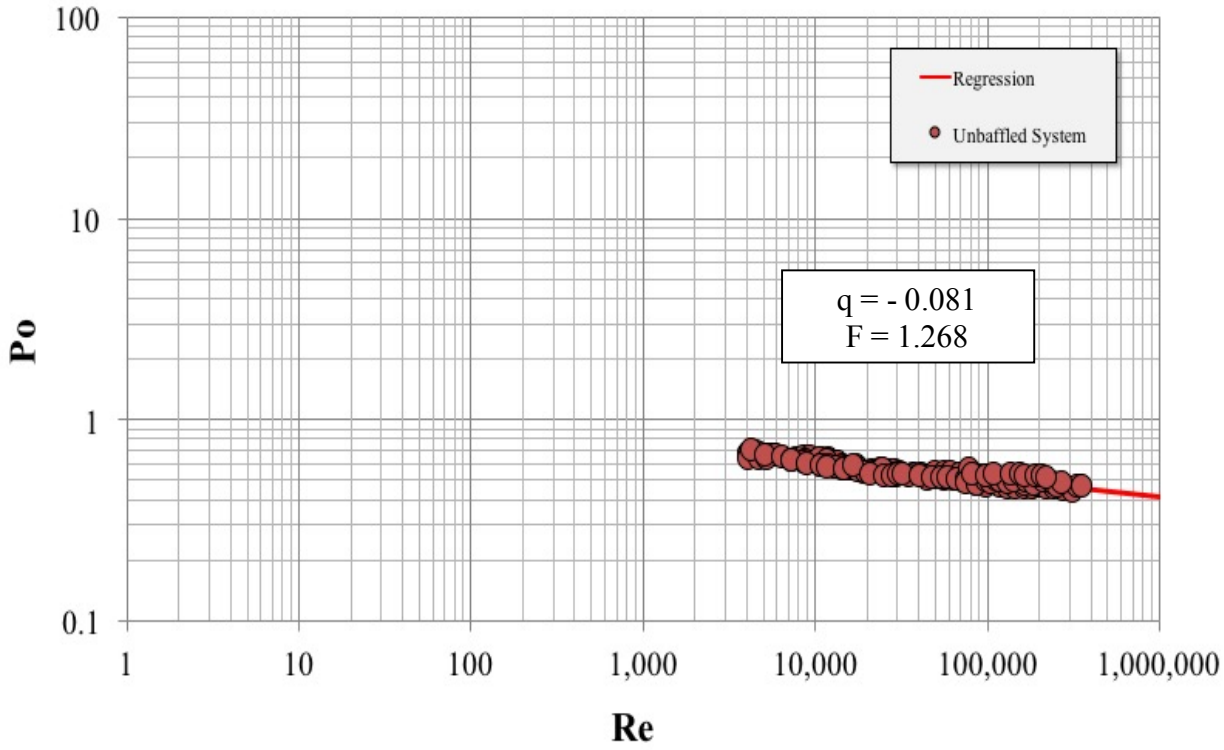

Figure 4.13 Correlation of *F* and *q* for retreat-blade impeller with partially baffled system.

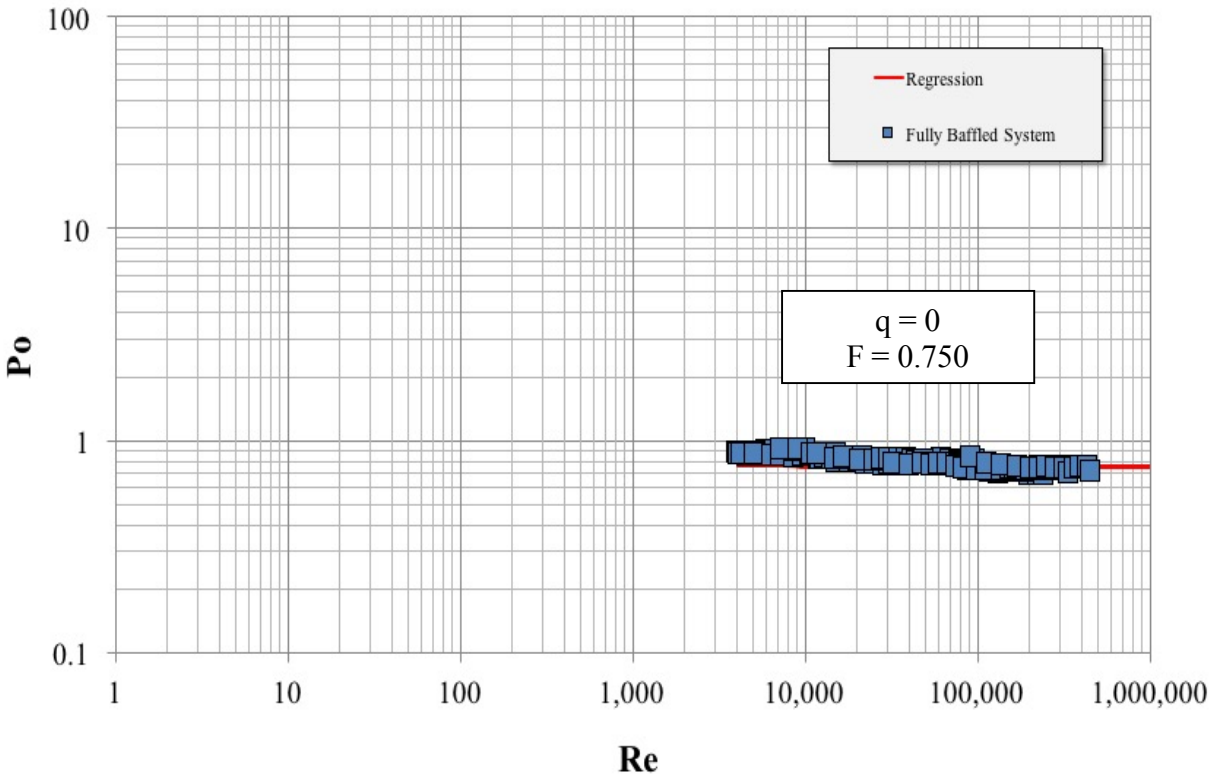

Figure 4.14 Correlation of *F* and *q* for retreat-blade impeller with fully baffled system.

Table 4.2 Summary of Coefficients *A*, *F*, and *q* and Their Standard Errors for Each Baffling Type Using the Modified Power-law Equation Approach

Baffling Type	A	F	q
Four-baffles	39.724 ± 0.256	0.750 ± 0.002	0
Beavertail baffle	39.724 ± 0.256	1.268 ± 0.013	-0.081 ± 0.003
No baffle	39.724 ± 0.256	3.143 ± 0.019	-0.211 ± 0.004

4.3.2 Comparison between Experimental Data and Prediction Bases on Correlating Equations

Figures 4.15 and 4.16 present a comparison of the experimental Po-Re data for the RBI with the predictions the modified Nagata correlation equation and the power-law correlation equation using the parameters in Tables 4.1 and 4.2, respectively.

The correlating equations with approximate coefficients based on modified Nagata equation for fully baffled, partially baffled and unbaffled vessels are, respectively:

$$Po = \frac{40}{Re} + 0.75 \tag{4.6}$$

$$Po = \frac{40}{Re} + 0.75\left(\frac{1000 + 1.2\,Re^{0.66}}{1000 + 3.2\,Re^{0.66}}\right)^{0.52} \tag{4.7}$$

$$Po = \frac{40}{Re} + 0.75\left(\frac{1000 + 1.2\,Re^{0.66}}{1000 + 3.2\,Re^{0.66}}\right)^{1.26} \tag{4.8}$$

When these correlations were used to predict the Po values for Re values in the Re range experimentally investigated in this work, the average deviations between the predicted values and the actual experimental data for fully baffled, partially baffled and unbaffled systems were found to be 7.52%, 5.33% and 8.24%, respectively. These results and the Figure 4.15 show that the values obtained from the correlations were in substantial agreement with the measured ones over the wide range of Re (about 6 orders of magnitude), for different flow regimes, from very laminar to highly turbulent. This was especially so

for the partially baffled system, the most relevant for industrial applications. The agreement was still satisfactory but not at good for the baffle and unbaffled systems.

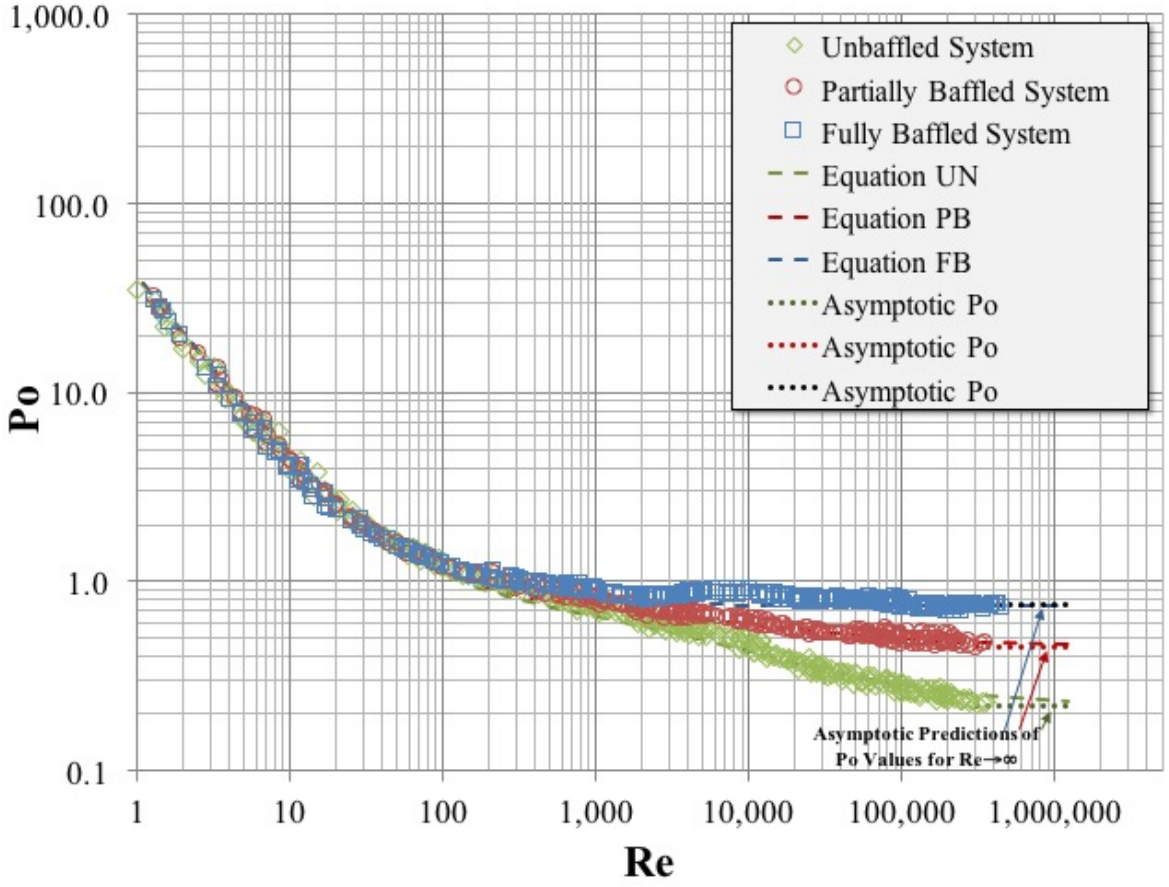

Figure 4.15 Comparison of the experimental results with the correlating equations based on the modified Nagata equation for different baffling configurations.

Similarly, the correlating equations with approximate coefficients based on the power-law equation for fully baffled, partially baffled and unbaffled vessels are, respectively:

$$Po = \frac{40}{Re} + 0.75 \tag{4.9}$$

$$Po = \frac{40}{Re} + 1.27Re^{-0.08} \tag{4.10}$$

$$Po = \frac{40}{Re} + 3.14Re^{-0.21} \tag{4.11}$$

When these power-law-based correlations were used to predict the Po values for Re values in the Re range experimentally investigated in this work, the average deviations between the predicted values and the actual experimental data for fully baffled, partially baffled and unbaffled systems were found to be 7.52%, 5.09% and 14.13%, respectively. These results and Figure 4.16 show that the values obtained from power-law based correlations were also in substantial agreement with the data. Again, this was especially so for the partially baffled system, satisfactory for the baffle system, but less so for the unbaffled system. The reason for the larger error for the unbaffled cases can be attributed to the larger deviation between data and correlation equation in the region for 10<Re<100.

The results presented in this section show that the two different types of correlating equations both resulted in adequate predictions of the experimental data. For the fully baffled and partially baffled systems both approached worked equally well, based on the average errors of the estimates. However, for the unbaffled system the modified Nagata equation was clearly superior to the power-law equation. In addition, the modified Nagata equation had the additional conceptual advantage of predicting that the Power Numbers have asymptotic limits for Re→∞, also shown in Figure 4.15, which makes more physical sense, although this may not have any practical impact since the range of Reynolds number covered in this work was quite extensive.

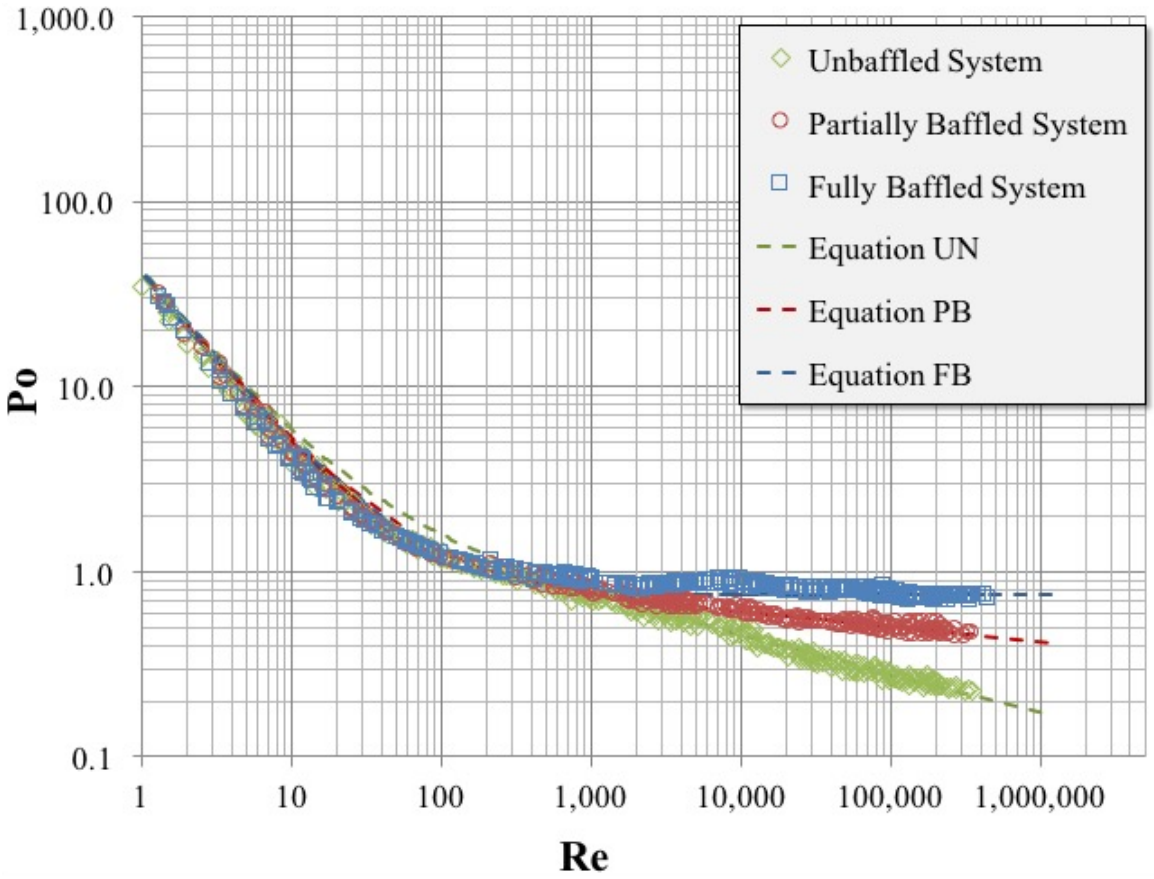

Figure 4.16 Comparison of the experimental results with the correlating equations based on the power-law equation for different baffling configurations.

The result of this work can be compared with the few results available in the literature. The results obtained here for the partially baffled case are in close qualitative agreement with the curve reported by Hemrajani et al. [13], for an RBI in a vessel equipped with a single finger baffle. However, no experimental points were reported in their work, and the curve was of unknown origin. In 2002, Campolo et al. [4, 5] generated experimental results as well as numerical results for an RBI in a system equipped with two beavertail baffles, and reported that Po at high Re was between 0.819 and 0.830 in a large scale system and about 9.7 in a lab-scale system. They also reported that these values were in closed agreement with those calculable by using one of Nagata's Equation [9]. In 2012, Furukawa et al. obtained results in a small flat-bottom tank, and obtained results that were similar (as

discernible from their figures) to those reported here for the high-Re value of Po in the fully baffled system and in the unbaffled system.

In summary, the results obtained in this work are similar to those reported by the few investigators who worked with a similar system, although such comparison can only be made for the few cases examined in previous studies.

CHAPTER 5

CONCLUSIONS

In this work the power dissipation, P, and the impeller Power Number, Po, were obtained in torispherical-bottomed vessel equipped with a retreat blade impeller under different baffling conditions. The experimental data were used to generate Po-vs.-Re plots for different baffling conditions and flow regimes ($0.5<Re<400,000$).

A number of conclusions can be drawn from these results:

- The data in the laminar region ($Re<10$) for different type of baffling were superimposable, indicating that the presence or absence of baffles in this region is unimportant as far as Po is concerned
- The data for different baffling types started to diverge when $Re>100$. The data for the fully baffled system at high Re shown a linear asymptote. The Po data for the partially baffled system and unbaffled system showed instead a decreasing trend with increasing Re values
- These results followed the typical relationships expected for a radial impeller
- Correlation equations were obtained to predict Po as a function of Re using two methods and a minimum number of independently obtained experimental parameters

- The correlating equation were typically in good agreement with the experimental data over a large range of Re
- In general, good agreement was observed between the experimental results and the correlating equations
- These results obtained here are of practical applicability to industrial systems, such as glass-lined vessels, typically used in the pharmaceutical and fine chemical industries, as long as geometric similarity is maintained

APPENDIX A - CALIBRATION DATA

The Appendix provides the power consumption data at varies agitation speed in order to obtain the appropriate calibration equation, as shown in the Table A.1

Table A.1 The Experimental Power Consumption at Varies Agitation Speed

N (RPM)	P_H (W)	β
20	0.141999988	3.632403166
20	0.205669599	3.225270519
20	0.277716791	7.669759318
20	0.299707939	6.819325809
20	0.368613538	8.557054673
20	0.415527988	7.950851113
20	0.848020577	8.88639086
30	0.761836218	0.63134062
30	0.91106187	1.272814816
30	1.091389288	1.637336223
30	1.992398061	5.271082178
40	0.973055965	2.099780092
40	1.443457105	3.777521012
40	1.774371531	4.523825358
40	2.083504248	4.727264283
40	3.501828611	5.413982517
50	1.577603111	2.538781069
50	2.357765287	4.541364405
50	2.812249024	5.480239302
50	3.275110341	6.182956833
50	5.320810758	5.849526633
50	9.253561161	3.541542906
60	2.278911311	3.399416586
60	3.460778467	4.220713177
60	3.977256299	7.373266354
60	4.60997306	4.873259284
60	6.89768083	5.157924504
60	8.313910798	2.971010966
70	2.828061707	5.956917165
70	4.824124959	4.992864881
70	5.635598342	4.945538017
70	6.525506821	6.07042779
70	11.28439137	4.771357267
70	14.6585666	2.748654824
80	0.605699064	5.760936162

N (RPM)	P_H (W)	β
80	1.063114954	3.438484793
80	4.521380147	6.723143002
80	6.3032915	6.248743213
80	7.277604102	5.963389766
80	8.244376881	5.845973879
80	10.21310828	5.386036334
90	4.924446485	6.858101039
90	8.233486027	6.289243363
90	9.632123076	6.047544446
90	15.31243675	5.13042607
100	1.414763892	10.67111687
100	5.697801876	7.522604914
100	10.18399619	6.257797067
100	11.67206391	5.951356161
100	13.48476287	5.667931582
100	17.60653243	5.134955309
110	2.042349384	2.851452173
110	8.677393068	5.610244087
110	12.35892078	5.094127811
110	14.46692945	5.008253842
110	16.41942928	4.924840576
110	20.81975339	4.667618234
120	0.973893723	7.448993222
120	2.413999795	8.012105278
120	2.718105964	8.019960922
120	8.898247032	6.963966787
120	14.55688372	5.886124371
120	16.72458265	5.718751668
120	18.87091875	5.634390474
120	24.29582095	5.02106538
120	25.23829874	3.834891044
130	1.293288976	2.572435465
130	3.302651637	5.774340863
130	8.955005139	8.70769864
130	15.82032757	7.019591916

N (RPM)	P_H (W)	β
130	20.57826964	4.724500058
140	1.596557387	4.636952863
140	3.811799086	9.054226254
140	4.244291675	7.857549635
140	5.625335806	10.92806218
140	10.59386931	6.646303373
140	13.59052982	7.744217441
140	17.3964646	5.435963124
140	24.74883861	4.95268248
140	27.02125729	4.706563776
150	1.724734367	4.91134373
150	4.737521722	7.589058151
150	5.215043805	5.086480669
150	10.1787602	6.69698263
150	18.26679048	5.228502054
150	24.87827222	4.744572957
150	28.96548427	4.763896648
150	31.8180504	3.591513591
160	2.536731348	8.234835437
160	6.259728082	5.131531494
160	11.37005213	6.537506245
160	16.0346889	5.692851926
160	18.32176836	5.295185625
170	2.408659088	3.90345454
170	6.638499436	8.390669745
170	7.211735376	4.53030522
170	12.99572161	5.94371296
170	18.89364294	5.319816114
170	26.30476473	4.829639364
170	31.64547224	4.586367838
180	1.685150299	1.091813628
180	3.049858148	3.418449214
180	8.063840023	7.7004997
180	8.849866505	7.815841001
180	16.15783934	5.611831169
180	23.42999801	4.97196794
180	28.76819225	4.766193651

N (RPM)	P_H (W)	β
180	35.30898815	4.126404986
190	8.889869452	8.249306161
190	10.15729265	7.708524105
190	37.38599978	4.119778083
200	2.029468854	4.440627191
200	3.489262241	8.955066655
200	10.50548583	8.678553099
200	12.19566268	3.644552415
200	20.71147317	5.971409288
200	26.28465854	5.287424461
200	34.00669328	5.324883274
200	39.63223852	4.253939571
220	2.395987997	5.127237825
220	7.994306106	9.282230182
220	13.13416113	8.137701853
220	18.79237894	7.171050932
220	24.87680615	6.112214903
220	36.99497621	5.634045495
220	46.00066571	3.262549066
230	10.08220858	9.492180296
230	14.87282322	7.970623745
230	19.78868269	7.356463983
230	28.36313623	5.865443622
230	37.08932871	5.772310704
240	38.48576664	5.60262545
240	47.91557115	3.571258374
250	3.008074966	3.755027234
250	14.4984501	10.6954874
250	22.10372231	7.707017235
250	36.39796889	6.248126431
250	46.23900787	4.816133021
260	7.528303196	8.296448592
260	20.05278591	7.619161244
260	25.56083559	7.026313386
260	27.83430147	6.630698207
260	33.98218885	6.606052231
280	3.521515925	8.255338923

N (RPM)	P_H (W)	β
180	31.72380262	5.060293066
280	18.63090107	8.636506205
280	25.18426335	8.04520912
280	30.95474073	7.232718519
280	41.87701119	6.762346992
280	48.97868611	5.406808765
300	4.517610236	7.078122004
300	6.927211801	8.850446853
300	17.05884811	9.304683885
300	23.80384754	8.466582811
300	28.27747547	8.467037756
300	38.20804985	3.224425617
300	49.68742941	6.100055138
300	62.38888851	3.291053169
320	9.379539027	8.763554063
320	16.69819327	10.83917702
320	23.84594488	9.771326463
320	32.26373767	9.017995237
320	36.7675249	7.395861173
320	44.54527055	6.95714586
320	66.49453123	1.427107998

N (RPM)	P_H (W)	β
280	11.86349162	9.972682749
350	14.52515363	10.50871065
350	18.03640702	12.20760307
350	33.84437766	10.69510682
350	38.6164569	10.67576736
350	44.34881629	7.777104318
350	64.68696353	4.145250171
360	30.05750187	9.65442218
360	43.52739453	7.536668576
360	47.157819	7.170499117
360	72.69896728	3.787664151
380	9.880727775	14.87615345
380	15.86965057	11.47176759
380	43.86438271	7.66407068
380	49.59066836	8.232640898
400	33.01604439	8.454058192
400	61.20241368	8.971829684
400	71.25551017	5.038080308
400	81.12011111	3.229012952

Summary of the linear regression

Regression Statistics	
Multiple R	0.657987008
R Square	0.432946903
Adjusted R Square	0.426681123
Standard Error	1.731599318
Observations	184

ANOVA

	df	*SS*	*MS*	*F*	*Significance F*
Regression	2	414.3661762	207.1830881	69.09704741	5.046E-23
Residual	181	542.7169518	2.998436198		
Total	183	957.083128			

	Coefficients	*Standard Error*	*t Stat*	*P-value*	*Lower 95%*	*Upper 95%*
Intercept	4.22448817	0.25683327	16.44836813	0.00000000	3.71771579	4.73126054
N (RPM)	0.02047801	0.00174669	11.72390288	0.00000000	0.01703152	0.02392450
P_H (W)	-0.09445914	0.01068460	-8.84068277	0.00000000	-0.11554153	-0.07337675

According to the statistics, the linear regression is as follows

$$Y = (4.2244817)X_1 + (0.02047801)X_2 - 0.09445914$$

$Y = \beta$ in %
X_1 = N in RPM
X_2 = P in Watts

REFERENCES

1. Armenate, P. M., & Chang, G. M. (1998). *Power Consumption in Agitated Vessels Provided with Multiple-Disk Turbines*. Industrial and Engineering Chemistry Research, 37, 284-291.

2. Banerjee, A. (2013). Power dissipation and mixing time in a partially filled pharmaceutical reactor equipped with a retreat-blade impeller at different fill ratios. MS Thesis, Otto H. York Department of Chemical, Biological and Pharmaceutical Engineering, New Jersey Institute of Technology, Newark, NJ.

3. Bates, R. L., Fondy, P. L., & Corptein, R. R. (1963). *An Examination of Some Geometric Parameters of Impeller Power.* Industrial and Engineering Chemistry Research, 2, 310-314.

4. Campolo, M., & Soldati, A. (2002). *Appraisal of Fluid Dynamic Efficiency of Retreated-Blade and Turbofoil Impellers in Industrial-Size CSTRs*. Industrial and Engineering Chemistry Research, 41, 1370-1377.

5. Campolo, M., Paglianti, A., & Soldati, A. (2002). *Fluid Dynamic Effiency and Scale-up of a Retreated Blade Impeller CSTR*. Industrial and Engineering Chemistry Research, 41, 164-172.

6. Dickey, D. S., Bittorf, K. J., Ramsey, C. J., & Johnson, K. E. (2004). *Understand Flow Patterns in Glass-lined Reactors*. Chemical Engineering Progress, 21-25.

7. Furukawa, H., Kato, Y., Inoue, Y., Kato, T., Tada, Y., Hashimoto, S. (2012). *Correlation of Power Consumption for Several Kinds of Mixing* Impellers. International Journal of Chemical Engineering, 1-6.

8. Harnby, N., Edwards, M. F., Nienow, A. W. (1985). *Mixing in the Process Industries Second Edition*. Oxford, UK: Reed Educational and Professional Publishinf Ltd.

9. Holland, F. A., Chapman, F. S. (1996). *Liquid Mixing and Processing in Stirred Tanks*. New York, NY.: Reinhold Publishing Corporation.

10. Myers, K. J., Reeder M.F., Fasano, J. B. (2002). *Optimize Mixing by Using the Proper Baffles*. Chemical Engineering Progress, 98(2), 42-47.

11. Nagata, S., Yokoyama, T., & Maeda, H. (1956). *Studies on the Power Requirement of Paddle Agitators in Cylindrical Vessels*. Kagaku Kogaku, 20, 582–592.

12. Oldshue, J. Y. (1983). *Fluid Mixing Technology*. New York, N.Y.: Chemical Engineering McGraw-Hill Publications Co.

13. Paul, E. L., Atiemo-Obeng, V. A., Kresta, S. M. (2004). *Handbook of Industrial Mixing: Science and Practice*. Hoboken, N.J.: John Wiley & Sons, Inc., 345-364.

14. Rushton, J. H, Costich, E. W., & Everett, H. J. (1950). *Power characteristics of mixing impellers Part II*. Chemical Engineering Progress, 9, 467–476.

15. Scargiali, F., Busciglio, A., Grisafi, F., Tamburini, A., & Micale, G. (2013). *Power Consumption in Uncovered Unbaffled Stirred Tanks: Influence of the Viscosity and Flow Regime.* Industrial and Engineering Chemistry Research, 52, 14998-15005.